RPSEA-0006-04 GRI-04/0186

IMAGING DEEP GAS PROSPECTS USING MULTICOMPONENT SEISMIC TECHNOLOGY

FINAL PROJECT REPORT

(January – September 2004)

Prepared by:

Bob A. Hardage (PI), Milo Backus, Michael DeAngelo, Sergey Fomel, Khaled Fouad, Robert Graebner, Paul Murray, and Randy Remington

Bureau of Economic Geology
John A. and Katherine G. Jackson School of Geosciences
The University of Texas at Austin
Austin, Texas 78713-8924

Prepared for:

RESEARCH PARTNERSHIP TO SECURE ENERGY FOR AMERICA
Subcontract No.

RPSEA Project Manager
Robert W. Siegfried
Vice-President, Unconventional Gas Technology

September 2004

LEGAL NOTICE

This report was prepared by the Bureau of Economic Geology at The University of Texas at Austin as an account of work sponsored by Research Partnership to Secure Energy for America (RPSEA) and Gas Research Institute (GRI). Neither RPSEA, members of RPSEA, GRI, members of GRI, nor any person acting on behalf of either:

a. MAKES ANY WARRANTY OR REPRESENTATION, EXPRESS OR IMLIED WITH RESPECT TO ACCURACY, COMPLETENESS, OR USEFULNESS OF THE INFORMATION CONTAINED IN THIS REPORT OR THAT THE USE OF ANY INFORMATION, APPARATUS, METHOD, OR PROCESS DISCLOSED IN THIS REPORT MAY NOT INFRINGE PRIVATELY OWNED RIGHTS, OR

b. ASSUMES ANY LIABILITY WITH RESPECT TO THE USE OF, OR FOR ANY AND ALL DAMAGES RESULTING FROM THE USE OF, ANY INFORMATION, APPARATUS, METHOD, OR PROCESS DISCLOSED IN THIS REPORT.

ANY DATA, CALCULATIONS, OR CONCLUSIONS REPORTED HEREIN SHOULD BE TREATED AS PRELIMINARY.

Reference to trade names or specific commercial products, commodities, or services in this report does not represent or constitute an endorsement, recommendation, or favoring by RPSEA, GRI or its contractors of the specific commercial product, commodity or service.

REPORT DOCUMENTATION PAGE

Form Approved
OMB No. 0704-0188

1. AGENCY USE ONLY (Leave blank)

2. REPORT DATE
September 30, 2004

3. REPORT TYPE AND DATES COVERED
Final report: January 2004–September 2004

4. TITLE AND SUBTITLE
Imaging Ultra-Deep and Overpressured Gas Prospects

5. FUNDING NUMBERS
RPSEA Subcontract R-521
GRI Contract 8693

6. AUTHOR(S)
Bob A. Hardage (Principal Investigator), M. Backus, M. DeAngelo, K. Fouad, R. J. Graebner, P. Murray, R. Remington

7. PERFORMING ORGANIZATION NAME(S) AND ADDRESS(ES)
Bureau of Economic Geology
John A. and Katherine G. Jackson School of Geosciences
The University of Texas at Austin
Austin, Texas 78713-8924

8. PERFORMING ORGANIZATION REPORT NUMBER

9. SPONSORING ORGANIZATION NAME AND ADDRESS
GRI
1700 S. Mt. Prospect Rd.
Des Plaines, IL 60018

10. SPONSORING/MONITORING AGENCY REPORT NUMBER
RPSEA-0006-04
GRI-04/0186

11. SUPPLEMENTARY NOTES

12a. DISTRIBUTION/AVAILABILITY STATEMENT

12b. DISTRIBUTION CODE

13. ABSTRACT (Maximum 200 words)
The objective of this research was to investigate the value of long-offset multicomponent seismic data for studying deep-gas geology across the northern shelf of the Gulf of Mexico (GOM). WesternGeco allowed the Bureau of Economic Geology to analyze some of their long-offset, four-component, ocean-bottom-cable (4-C OBC) seismic spec data so the research could be done. These data were processed using source-receiver offsets as large as 10 km. These data represent the largest imaging offsets available for seismic reflection data and should image deeper than conventional seismic reflection data. The P-P mode extracted from the data verifies that sediment accumulations 18 km (60,000 ft) thick occur beneath portions of the seismic grid. This information sets new guidelines for deep geology across the GOM basin. The P-SV mode sometimes images to depths of 13 km (42,000 ft). Previously, no one k new the depth-imaging capability of P-SV data. Both modes, P-P and P-SV, provide good images of geologic conditions to depths of 9 km (30,000 ft), the present deepest depth that most operators wish to drill along the shallow-water, northern shelf of the GOM.

14. SUBJECT TERMS

15. NUMBER OF PAGES

16. PRICE CODE

17. SECURITY CLASSIFICATION OF REPORT	18. SECURITY CLASSIFICATION OF THIS PAGE	19. SECURITY CLASSIFICATION OF ABSTRACT	20. LIMITATION OF ABSTRACT
Unclassified	Unclassified	Unclassified	

NSN 7540-01-280-5500

Standard Form 298 (Rev. 2-89)
Prescribed by ANSI Std. Z39-18
298-102

Table of Contents

Figures

SUMMARY
Long-offset four-component ocean-bottom-cable (4-C OBC) seismic data have been analyzed to determine whether increased source-receiver offsets improve the ability to image deeper geology across gas-producing areas of the northern Gulf of Mexico (GOM). In this study, the term *long offset* means that 4-C OBC data were processed using uniformly sampled source-receiver offsets that ranged from 0 to 10 km. Seismic data with 10-km offsets are rare, particularly across shallow-water areas where congested production facilities have developed over decades of exploration and development. The 4-C OBC data used in this study were acquired across a 3,200-mi^2 (8,200-km^2) area of the Louisiana shelf noted for prolific gas production. The P-P and P-SV images produced from these long-offset reflection data were interpreted to determine the relative depth-imaging capabilities of each seismic mode. In this study area, both P-P and P-SV data provided good-quality images of geology to depths of 9 km (30,000 ft), the present deepest drilling depth considered by operators along the GOM shelf. In areas of thickest sediment deposition, P-P reflections were observed from depths of 18 km (60,000 ft), and P-SV reflections returned from depths of 13 km (42,000 ft).

INTRODUCTION
Operators across the Gulf of Mexico (GOM) are targeting deeper and deeper drilling objectives. For deep targets to be evaluated, seismic data are required that have longer and longer source-receiver offsets. Most shallow-water operators in the GOM consider 30,000 ft (9 km) to be the deepest target depth that will be drilled for the next several years. For geology at depths of 9 km to be imaged, seismic reflection data must be acquired with offsets of 9 km or more.

This long-offset requirement is difficult to achieve using towed-cable seismic technology in areas that are congested with production facilities, which is the situation for many shallow-water blocks across the northern GOM shelf. Ocean-bottom-cable (OBC) and ocean-bottom-sensor (OBS) technologies are logical options for long-offset data acquisition in congested production areas because ocean-floor sensors are immobile, once deployed, and can be positioned quite close to platforms, well heads, and other obstructions that interfere with towed-cable operations. An example illustrating the deployment of ocean-floor sensors through a congested platform complex in part of the area of study is illustrated in Figure 1. A 10-km circle is positioned atop this map of production facilities to illustrate the difficulty of towing a 10-km cable across the area in any azimuth direction. In contrast, note that OBC lines AA and BB, which are real lines used in this study, pass within a few meters of several platforms.

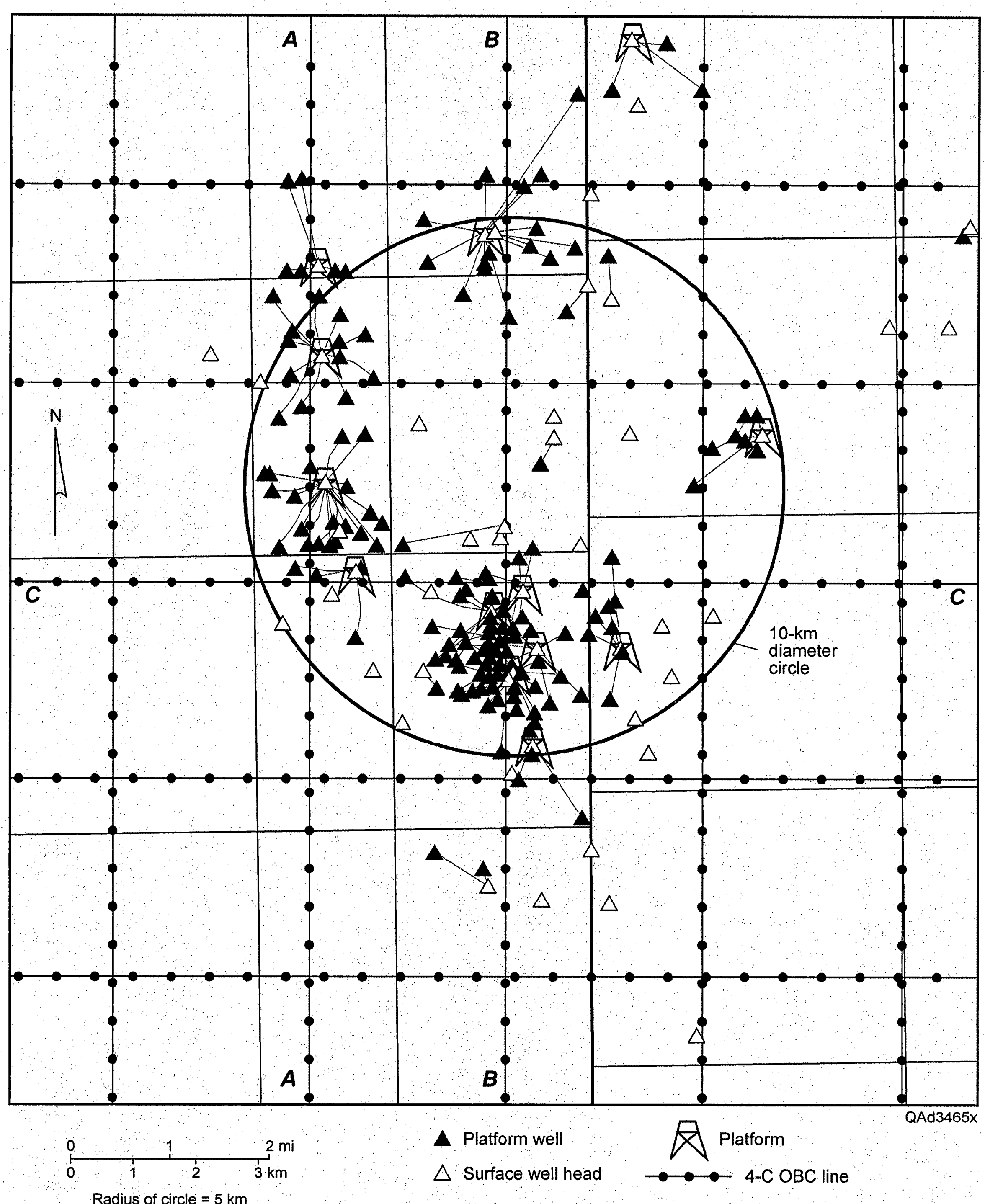

Figure 1. 4-C OBC data acquisition across congested areas.

An additional appeal of OBC seismic technology is that 4-C data can be acquired, allowing targeted reservoir intervals to be imaged with P-SV wavefields, as well as P-P wavefields. Once 4-C seafloor receivers are deployed, source boats can maneuver along a receiver line to generate P-P and P-SV data from long-offset distances. For the data used in this study, some field records were acquired with offsets greater than 10 km. However, data offsets were limited to 10 km during data processing. Several data examples will be illustrated and discussed that will document the imaging depths and image qualities of P-P and P-SV modes acquired with long-offset imaging strategies.

STUDY AREA

WesternGeco allowed access to some of its long-offset 4-C OBC seismic spec data for this study. The company has acquired a considerable amount of long-offset OBC data and segregates its spec-data programs into the four survey areas shown in Figure 2. Data used in this study came from the WesternGeco Shelf-B spec survey, which extends across the West Cameron South, East Cameron South, and Vermilion South areas of the GOM and portions of the West Cameron, East Cameron, and Vermilion areas. The data consisted of parallel north-south and parallel east-west 2-D profiles spaced at intervals of 2 mi. The east-west profiles were approximately 75 mi (120 km) long; the north-south profiles spanned approximately 45 mi (70 km).

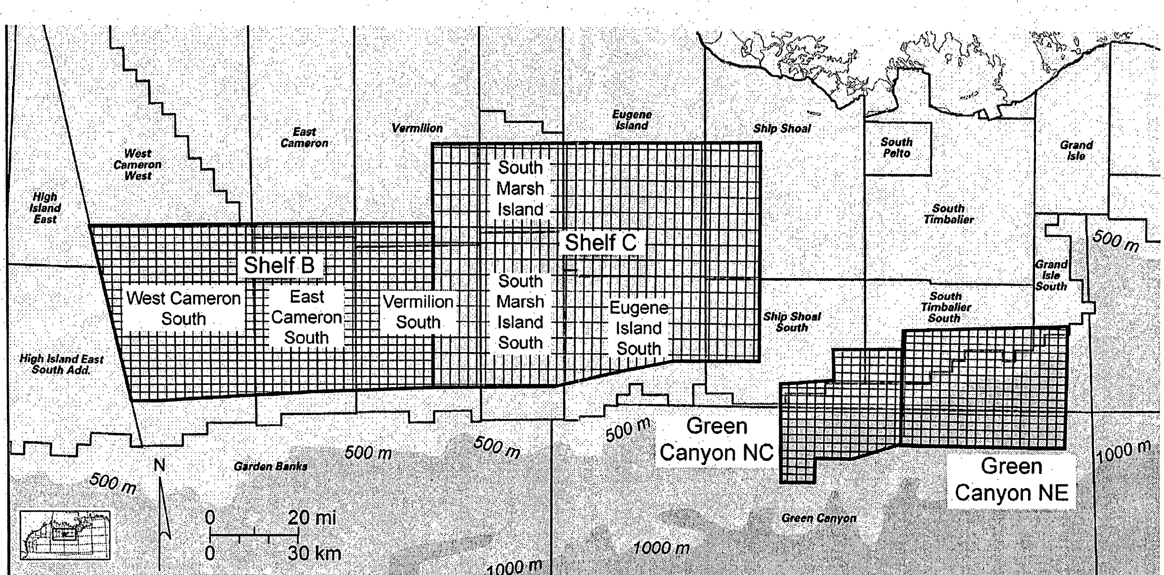

Figure 2. Location of WesternGeco's long-offset 4C2D seismic spec data surveys.

SEISMIC DATA PROCESSING

WesternGeco has a large financial investment in its long-offset 4-C OBC seismic spec data. To protect that investment and to ensure that the data remained fully in WesternGeco's control, only WesternGeco personnel processed the data that were interpreted. Processing procedures used to produce migrated P-P and P-SV images are listed in Figure 3. The interpretation demonstrated that image quality was good across the Shelf-B survey for both P-P and P-SV modes. Therefore, the data-processing strategies summarized in Figure 3 were robust procedures for these particular data and for this particular survey area. This statement will be supported by numerous data examples that follow.

P-P Data-Processing Sequence

1. Source-signature deconvolution
2. Spherical divergence correction
3. Sum hydrophone and vertical-geophone data
4. Deconvolution and Q compensation
5. Wavefield extrapolation to redatum sources and receivers (Kirchoff)
6. Pre-DMO velocity analysis (1 km)
7. Demultiple
8. DMO velocity analysis (1 km)
9. 4th order NMO (plus common-offset DMO if PSTM is not done)
10. Pre-stack time migration (Kirchoff)
11. Stack
12. Post-migration enhancement
13. Bandpass filter and scale data
14. Correct to sea level

P-SV Data-Processing Sequence

1. Source-signature deconvolution
2. Spherical divergence correction
3. Radial/transverse rotation
4. Application of S-wave receiver statics
5. Deconvolution and Q compensation
6. Wavefield extrapolation to redatum sources and receivers (Kirchoff)
7. CCP binning
8. Vp/Vs velocity analysis for positive offsets and negative offsets (2 km)
9. CCP stack (positive offsets and negative offsets stacked separately)
10. Vp/Vs velocity scans
11. Revision of S-wave receiver statics
12. Redoing of CCP binning (positive offsets and negative offsets stacked separately)
13. Azimuthal DMO velocity analysis for positive offsets and negative offsets (1 km)
14. 4th-order NMO; common-offset azimuthal DMO
15. Prestack time migration
16. Stack and inverse migration
17. Final poststack migration (finite difference or phase shift with stretch)
18. Enhancement, bandpass filter, and scale data
19. Correction to sea level

QAd3928x

Figure 3. Data-processing procedures used to construct P-P and P-SV seismic images.

DEEP GEOLOGY ACROSS THE AREA

In this discussion, the term *super deep* refers to the first strata that infilled the GOM basin as plate movements provided the initial accommodation space for sediment inflow. There are several published models of super-deep geology across the GOM basin. All of these models involve an element of conjecture because no wells yet penetrate super-deep strata underneath the GOM shelf, and existing seismic data rarely image super-deep structure or stratigraphy. It will be helpful, though, to summarize these models for a better appreciation of the deep-imaging capabilities of Shelf-B long-offset data.

The mechanism that many plate-dynamics researchers think created the GOM basin was an angular movement of the North American plate away from the South American and Caribbean plates relative to a rotation pole assumed to be located southeast of present-day Florida. This hypothetical rifting, or opening-scissors type of plate rotation, is shown in a generalized and simplified form in Figure 4. Such plate movement should produce basement-separation lineaments trending northwest-southeast across the GOM basin, as illustrated in this diagram.

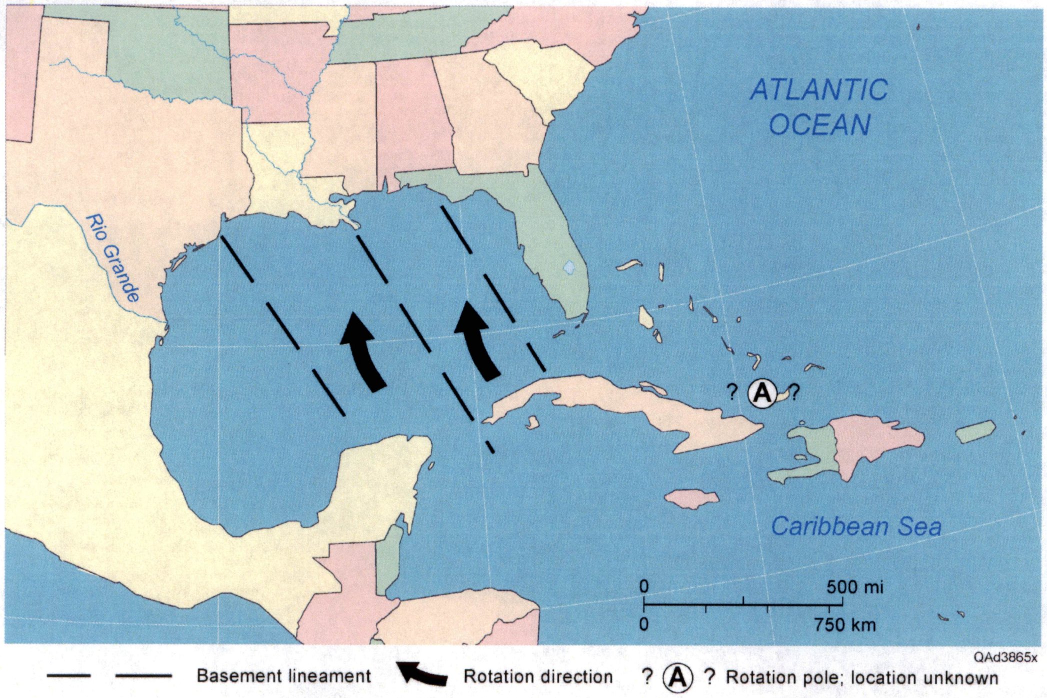

Figure 4. One model proposed for the opening of the GOM.

An authoritative description of present-day plate and basement tectonic features is the *Tectonic Map of the World* developed by Exxon Production Research Company (1985) and distributed by the American Association of Petroleum Geologists. The portion of this worldwide map that spans the GOM basin is shown in Figure 5, together with an indication of the location and size of the Shelf-B seismic survey area. A number of major lineaments do trend northwest-southeast across the GOM basin, as implied by the model in Figure 4. These northwest-southeast-trending lineaments indicate lateral expansion of the basin to the northeast and southwest. Lineaments trending northeast-southwest would indicate basin expansion to the northwest and southeast. No lineaments are defined beneath the large salt province north of the Sigsbee Deep, where deep, reliable geophysical data are difficult to acquire (Fig. 5). The lineament labeled "1" should traverse the Shelf-B survey area within this salt province if the linear feature continues on the trend shown on the map. A long, curving lineament oriented northeast-southwest traverses the Sigsbee Deep area of the basin. Other, shorter, northeast-southwest-trending lineaments occur normal to the long northwest-southeast lineaments as a result of crustal movements parallel to these long-lineament trends. One of these short lineaments is labeled "Orthogonal Lineament" in Figure 5. Such a northeast-southwest lineament possibly underlies the Shelf-B study area. Because the Shelf-B survey is positioned in a salt province where basement information needed to construct this tectonic map was sparse, the long-offset Shelf-B seismic data may provide the most definitive basement information available to date beneath the GOM salt province.

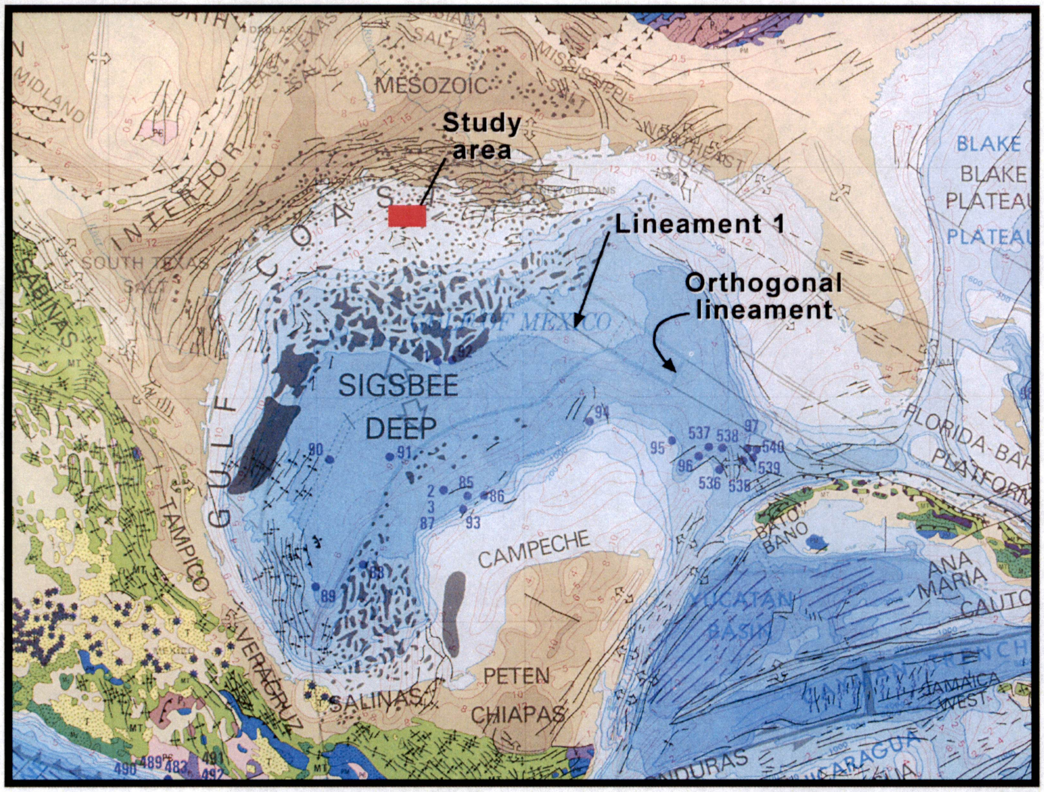

From Tectonic Map of the World: Exxon Production Research Co. and AAPG

QAd3880x

Figure 5. Plate and basement tectonic elements across the GOM modified from Tectonic Map of the World produced by Exxon Production Research Company (1985) and distributed by AAPG.

Several geological issues should be considered in order to establish a framework for evaluating the depth-imaging capability of long-offset seismic data in the GOM basin. Key questions that need to be answered would include:

1. How deep is the Moho beneath the Shelf-B area?
2. How thick is the sediment accumulation beneath the Shelf-B survey?
3. What is the conventional wisdom about the deepest depths that can be imaged with reflection seismic data available in the study area?

The issues of Moho and basement depths across the GOM basin were considered by Sawyer and others (1991). In their analysis, the Moho beneath the GOM basin was defined as "a layer in which P-wave velocity Vp exceeds 7.6 km/s," with the observation that Vp within the Moho is usually in the range of from 8.0 to 8.5 km/s. No unit was imaged with the long-offset data used in this study that had a seismic P-wave interval velocity significantly exceeding 5 km/s. Thus, the Shelf-B long-offset data do not contain Moho reflections, according to the Vp definition of Moho used by Sawyer and others (1991). The estimated depth to Moho across the GOM basin developed by Sawyer and others (1991) is reproduced as Figure 6. The location and physical size of the Shelf-B survey are indicated on the map. This map implies that Moho depth beneath the Shelf-B area is 25 to 30 km. Subsequent data examples will lead to the conclusion that the Shelf-B, P-P, long-offset data image to a depth of 18 km in some areas of the survey.

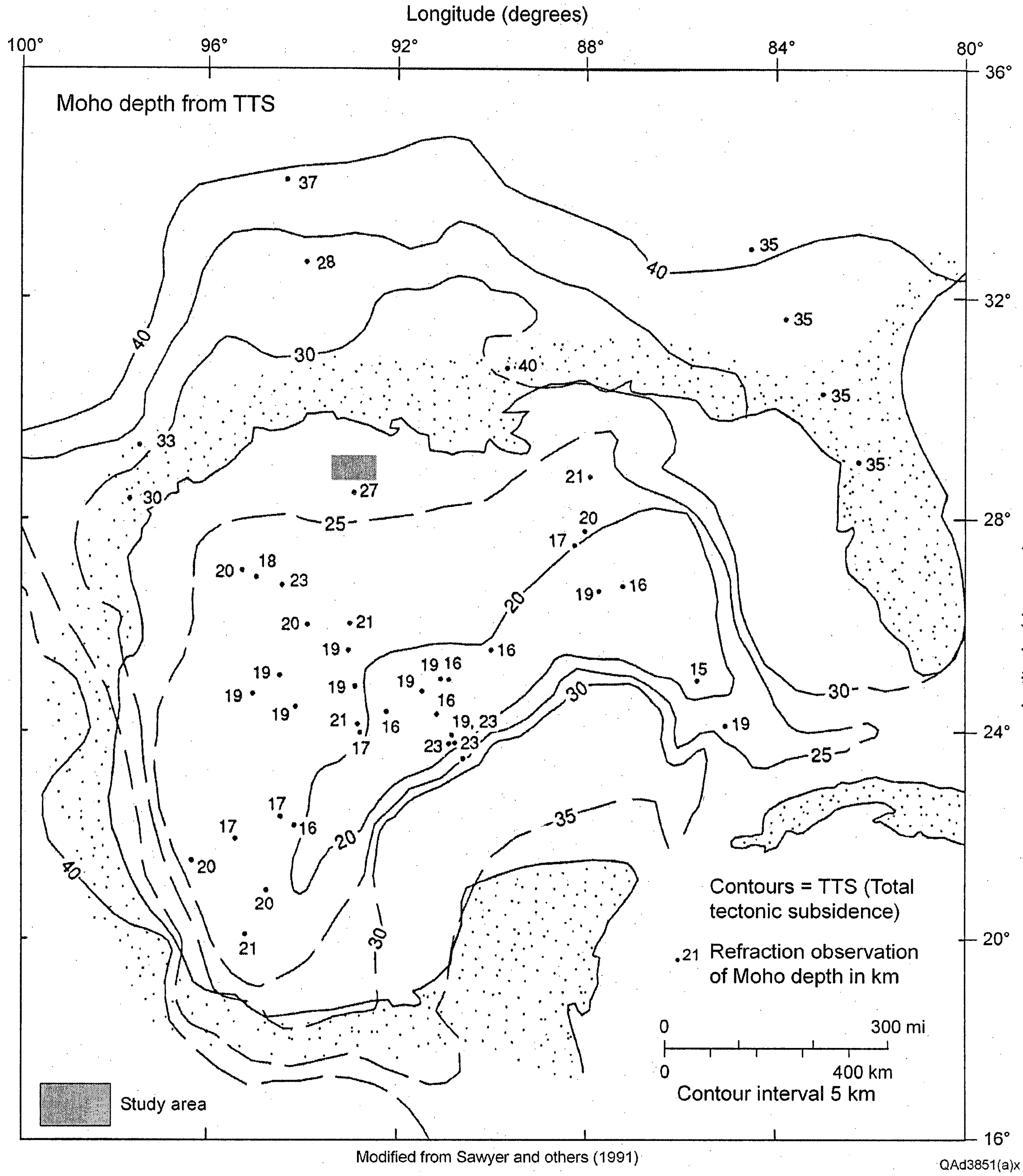

Figure 6. Estimated Moho depths across the GOM basin (modified from Sawyer and others, 1991).

Sawyer and others (1991) used a GOM-specific definition of seismic basement, which they stated as *rock beneath an unconformity at the base of the marine Mesozoic section that is overlain by Middle Jurassic salt (and equivalents) and younger rocks and underlain by Lower Jurassic and older rocks.* Other researchers may use a different definition of crustal basement. The map of basement depths and regional extents of crust types across the GOM basin that was published by Sawyer and others (1991) is shown in Figure 7, with the Shelf-B survey area highlighted. The labels *continental, oceanic, thick transitional,* and *thin transitional* refer to types of basement crust. Dashed contours are speculative basement depths. Depth contours in the vicinity of the Shelf-B survey are the deepest values on the map, but all of the contours in the survey area are dashed (speculative). Taken at face value, this map suggests basement depth beneath the Shelf-B survey to be about 15 or 16 km.

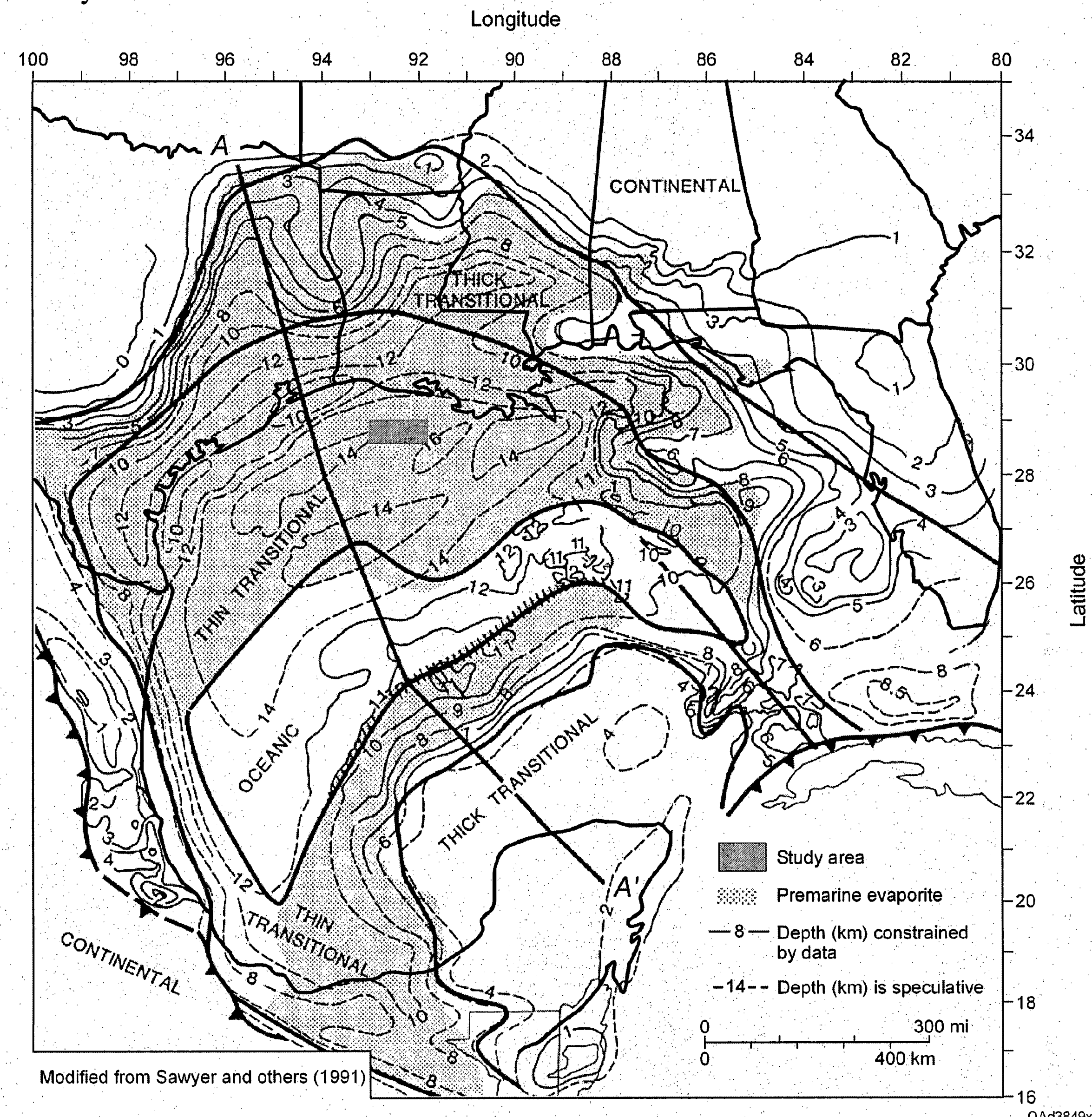

Figure 7. Depth to basement and types of basement crust across the GOM basin (modified from Sawyer and others, 1991).

Several cross-section profiles traversed the original basement-depth map published by Sawyer and others (1991). The map in Figure 7 eliminates all of these profile locations except profile A-A′, the closest traverse to the Shelf-B area. A reproduction of the published schematic cross section of the geology along A-A′ is shown as Figure 8. A labeled arrow identifies the location of the seismic study area. This cross section tells the same story as the basement-depth map (Fig. 7): the thickest sedimentary section in the GOM basin is beneath the Shelf-B survey, where the depth to basement is speculative but is probably at least 15 km.

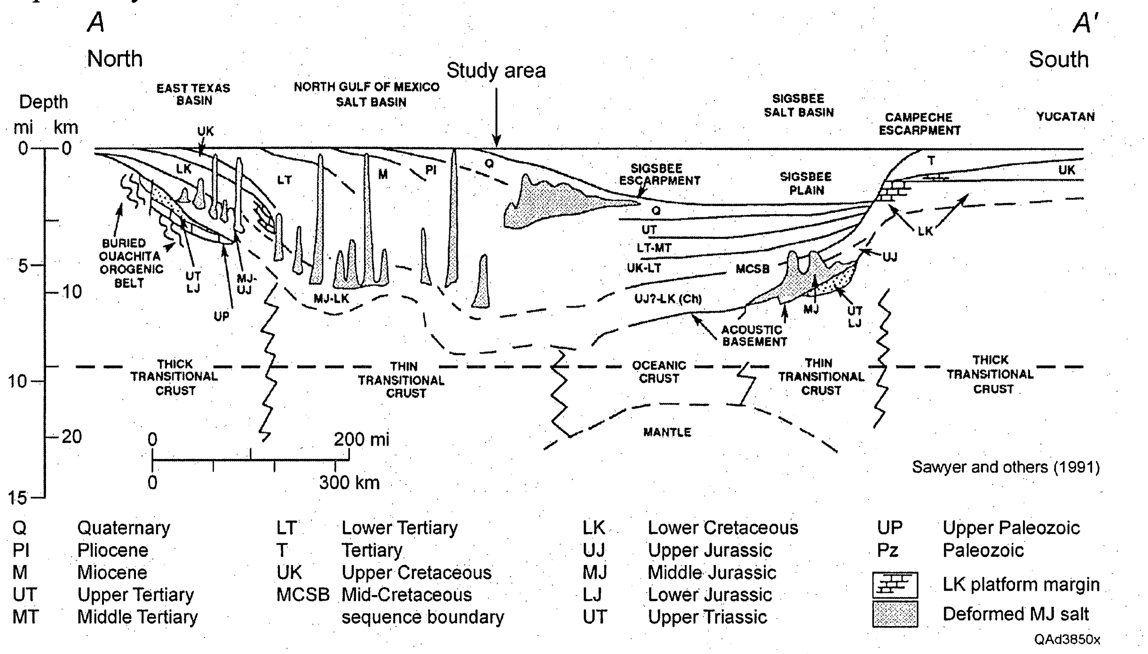

Figure 8. Schematic cross section of geology near the Shelf-B seismic survey (modified from Sawyer and others, 1991).

A similar cross section across the GOM basin was published by Galloway and others (1991). A modified version of their cross section is shown as Figure 9. The location of this cross section in the basin, as shown on the map inset, places the geology in the immediate vicinity of the Shelf-B survey. The position of the seismic survey is labeled on the cross section. This basin model also shows that the thickest sediment accumulation in the GOM basin is beneath the Shelf-B area, and that although the thickness of the sediment beneath the seismic survey is unknown, it is probably 15 km or more.

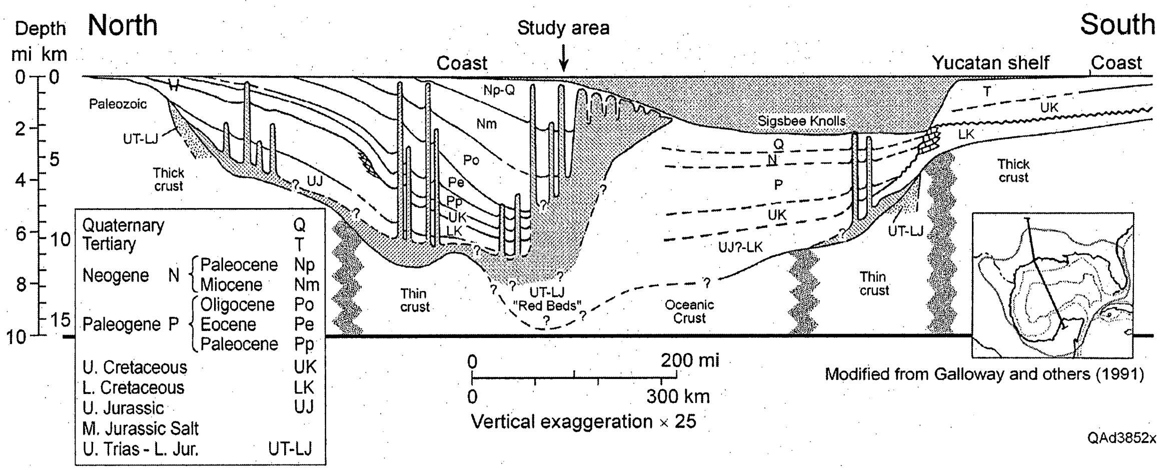

Figure 9. Generalized geologic cross section of the Gulf of Mexico basin in the vicinity of the seismic study area (modified from Galloway and others, 1991).

Two published studies have been selected to address the question of the maximum depths imaged by conventional seismic data across the northern GOM basin. The first selected study was done by Diegel and others (1995). Their map of the tectonic and stratigraphic provinces of the northern GOM basin is reproduced as Figure 10. The numbered traverses across the map represent locations where seismic lines are spliced together to make long, regional transects across the basin. Three of these seismic profiles (9, 11, and 17) traverse some portion of the Shelf-B survey. Profile 9 is displayed as Figure 11, profile 11 is shown as Figure 12, and profile 17 is reproduced in Figure 13. The position of the Shelf-B survey is labeled on each profile. These reflection data show that, at some locations along the profile, interpretable P-P reflections exist down to a maximum image time of 6 s. No doubt some GOM explorationists utilize seismic data that image deeper than 6 s, but a 6-s seismic basement is typical of most conventional seismic data across the northern GOM shelf. Later data examples will show that Shelf-B, long-offset, P-P data have reflection events at two-way traveltimes of 10 s.

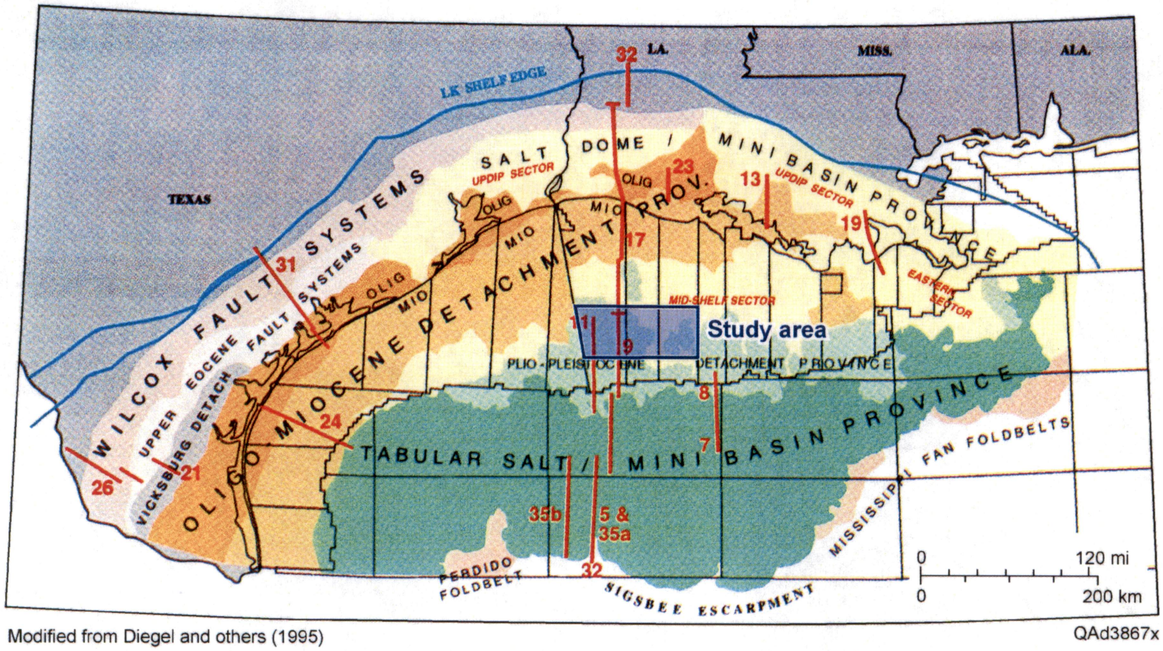

Figure 10. Tectonic and stratigraphic provinces of the northern Gulf of Mexico basin (modified from Diegel and others, 1995).

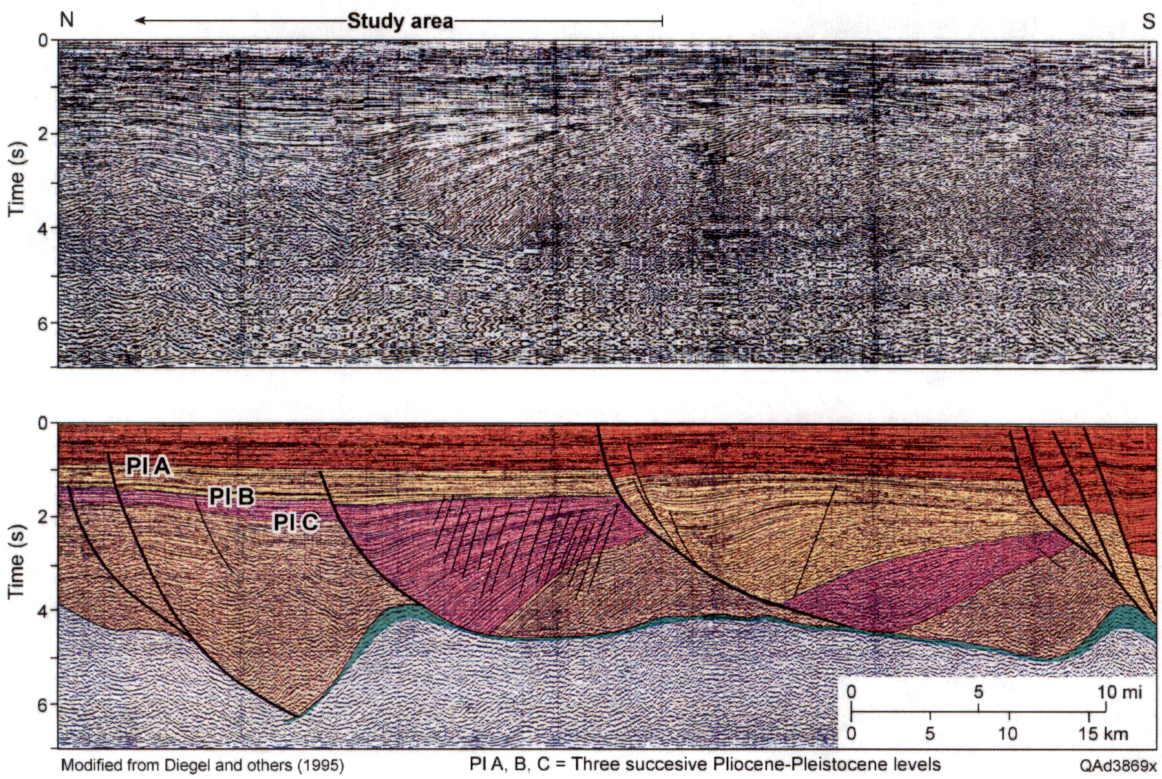

Figure 11. Seismic profile 9 traversing the study area. The location of the profile is defined in Figure 10 (modified from Diegel and other, 1995).

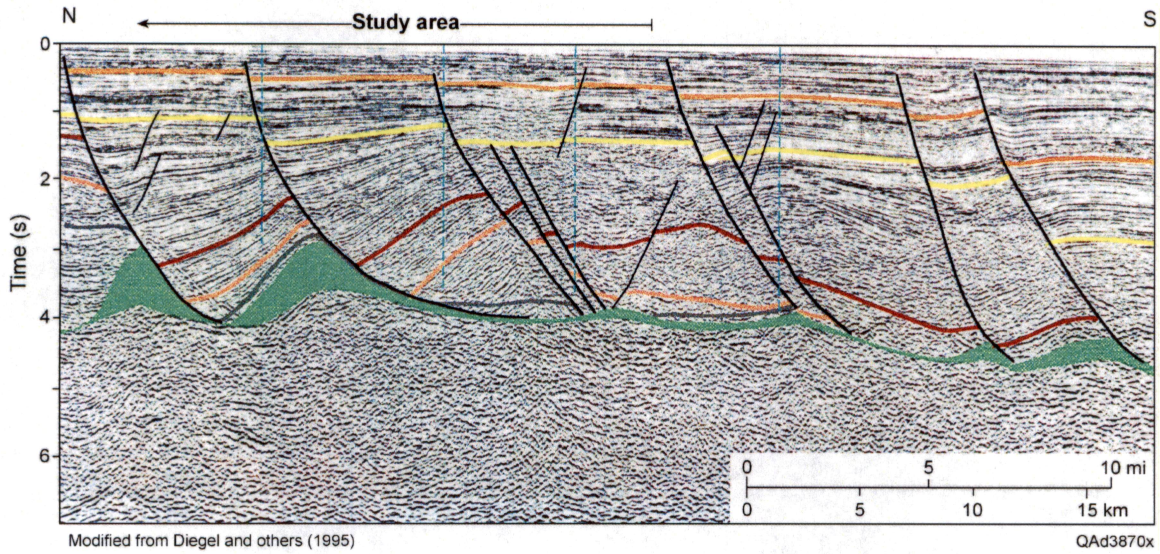

Figure 12. Seismic profile 11 traversing the study area. The location of the profile is defined in Figure 10 (modified from Diegel and others, 1995).

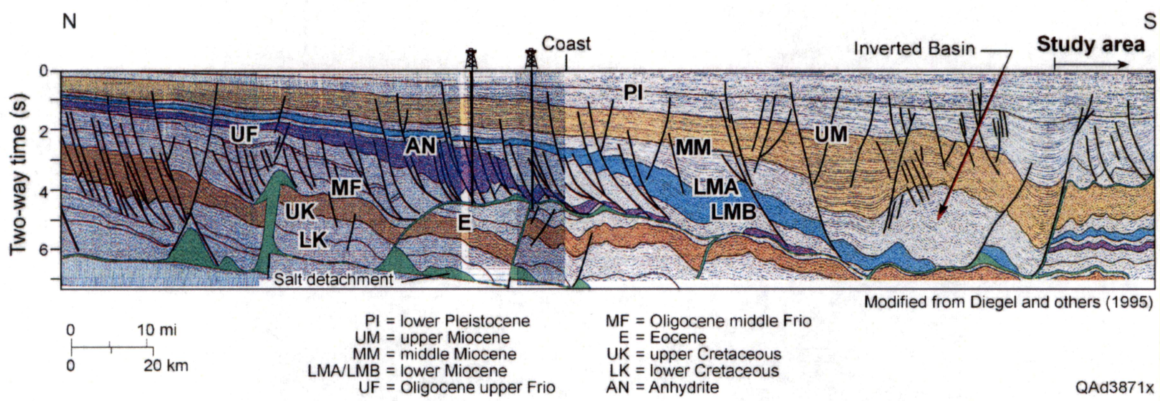

Figure 13. Seismic profile 17 traversing the study area. The location of the profile is defined in Figure 10 (modified from Diegel and others, 1995).

The second selected study was published by Peel and others (1995). They developed models of sediment thicknesses across the GOM basin along several traverses that started onshore, crossed the GOM shelf, and ended at the oceanic crust in the center of the basin. Their map of locations of these traverses is shown in Figure 14, together with a depositional model developed for profile 4 that crosses the Shelf-B study area. This profile is significant in two respects: it implies that sediment is 20 km thick beneath the Shelf-B survey, and it indicates that seismic data in the area image to depths of only 10 or 12 km.

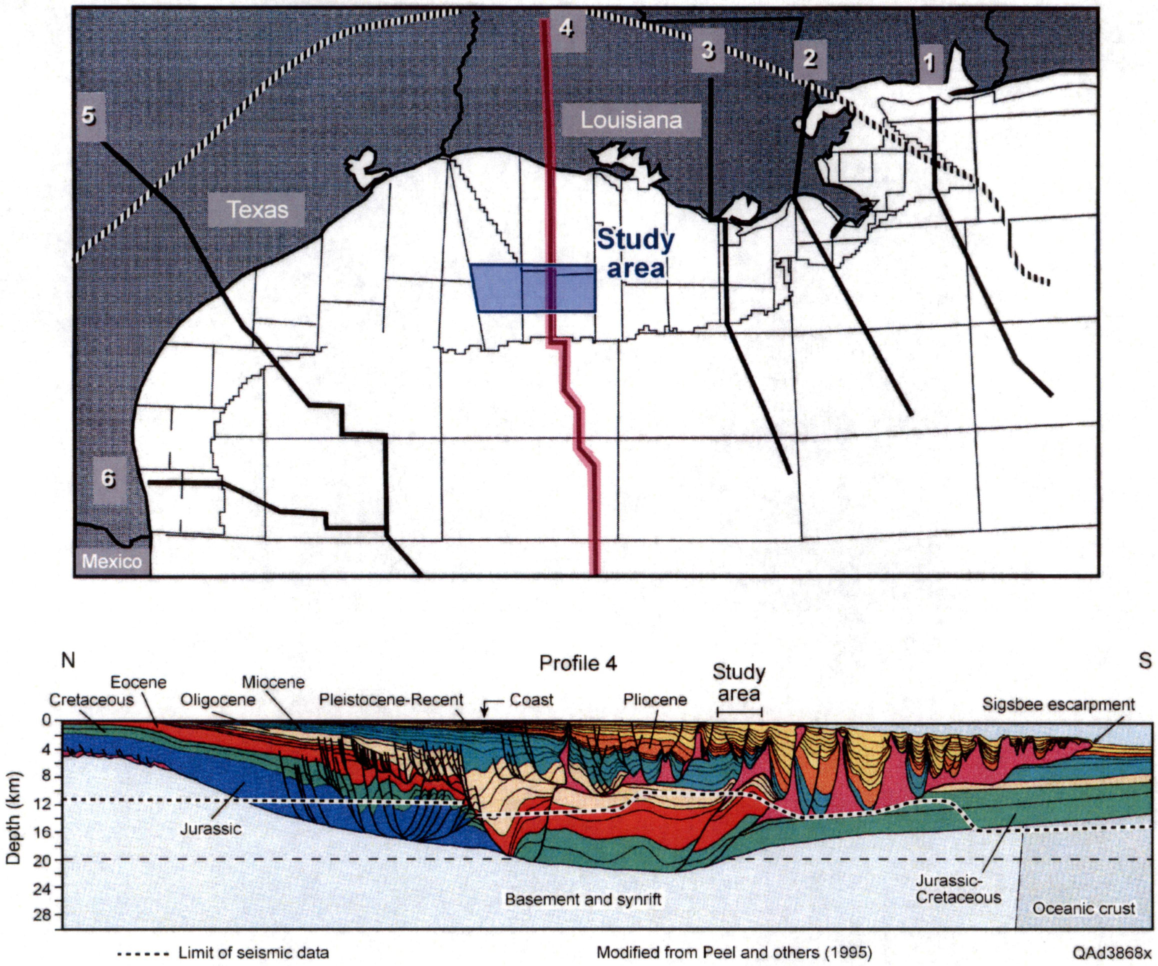

Figure 14. One proposed model of sediment thickness and maximum seismic imaging depths (modified from Peel and others, 1995).

Other published studies could be considered, but the ones presented here were done by respected scientists and can be viewed as "conventional wisdom" of the deep geology beneath the Shelf-B survey area. Key concepts provided by these studies can be summarized as

- The sediment accumulation in the GOM basin is thickest in the area of the Shelf-B survey,
- The sediment beneath the Shelf-B survey is thought to be 15 to 20 km thick,
- Most P-P seismic reflection data image geology to a maximum two-way time of about 6 s, and
- The depth to Moho is 25 to 30 km in the Shelf-B area.

No studies were found that illustrate or interpret converted-SV (P-SV) seismic reflection data across the GOM basin. For this reason, the long-offset P-SV data examples that follow will be valuable indications of the imaging capabilities of this important seismic wave mode across GOM-basin plays.

SEISMIC INTERPRETATION PROCEDURE

The depth-imaging ability of the 10-km offset 4-C OBC data used in this study will be illustrated using profiles that extend the full north-south and east-west extents of the Shelf-B survey. Two horizons were interpreted along these profiles. Neither horizon is a structural horizon, which is a crucial point. Rather, each horizon is only a convenient and subjective marker that indicates seismic reflection quality. Horizon 1, the shallower horizon, marks the *base of continuous reflections*. As such, that horizon crosses geologic time lines and does not map structure or indicate depth variations of a fixed formation. Horizon 2, a deeper horizon, defines the *base of discontinuous, but mappable reflections*. This horizon also crosses geologic time lines and follows no fixed geologic structure. When the following interpreted data are inspected, Horizons 1 and 2 must be viewed only as indicators of seismic reflection quality, never as geologic-time surfaces.

LONG-LENGTH SEISMIC PROFILES

Image quality of long-offset Shelf-B data will be illustrated along three profiles that traverse the full east-west and north-south dimensions of the Shelf-B survey. The first example is a north-south profile in the west part of the survey. The P-P image along this profile is displayed in Figure 15. The profile is 45 mi (72 km) long, and a 10-km scale bar is positioned on the image to represent the dimension of the longest source-receiver offset used in processing the data. This maximum-offset scale bar can be compared with the physical sizes of the salt structures and rotated fault blocks along the profile to identify locations where the seismic propagation velocity can be expected to change over lateral distances similar to the maximum offset and have a significant effect on deep imaging.

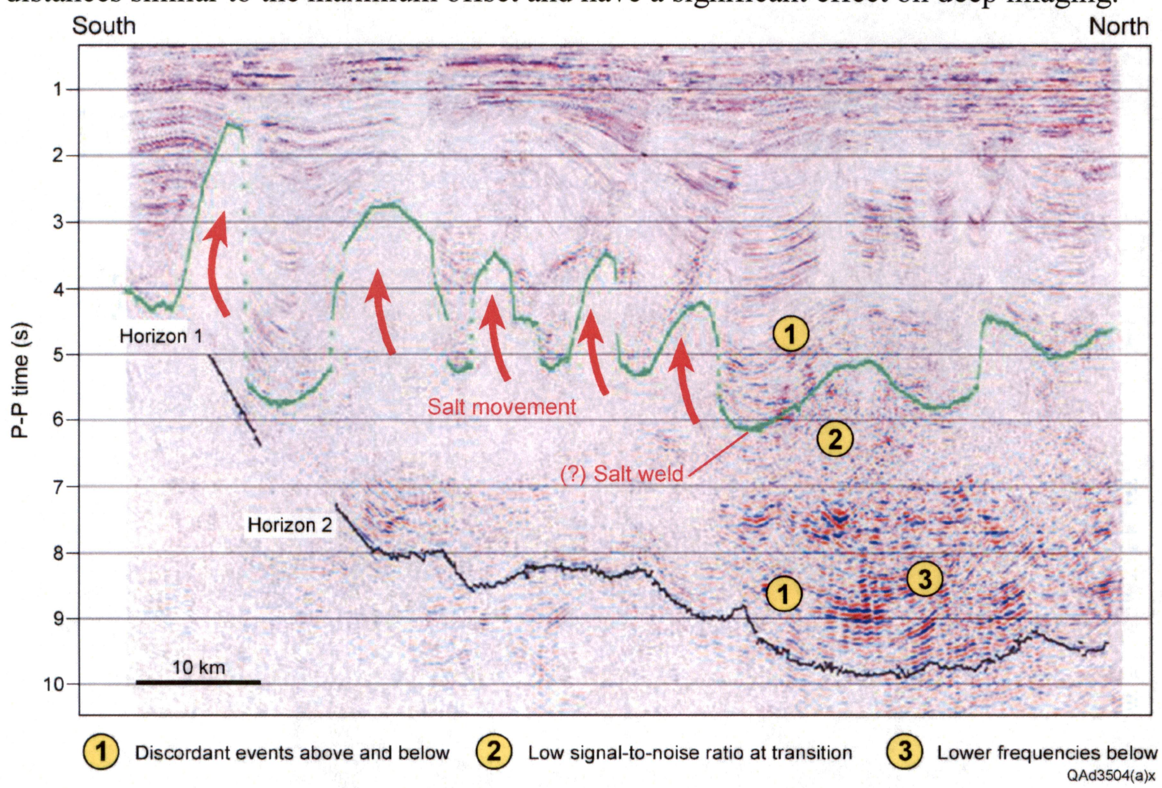

Figure 15. P-P image from the west portion of the Shelf-B survey.

The profile shows that there is a huge sediment accumulation in the northern one-third of the image space, where Horizon 2 drops down to approximately 10 s. This sediment load squeezes the Jurassic salt southward, causing several salt structures to punch upward through overlying, younger strata, as shown by the salt-flow arrows. This salt movement creates numerous en echelon, rotated fault blocks. The depth of shallower Horizon 1 is controlled to a great extent by the vertical depth to the tops of the various salt structures along the profile. The definition of the base of continuous reflections (Horizon 1) in the north part of the profile is arbitrary. If desired, Horizon 1 could be positioned at the north end of the seismic line deeper than where it is shown in Figure 15. The exact vertical position of Horizon 1 in P-P image space is not too critical because the surface is a data-quality indicator, not a geologic horizon.

The 10-s-image times of the deepest P-P reflections on this profile are considerably deeper than the maximum P-P seismic imaging depths observed with "conventional" seismic data in the area (Figs. 11 through 14). Interpreters have to acknowledge that these long-offset data image much deeper geology than do seismic reflection data acquired to date over the northern GOM shelf.

In the north part of this profile, a salt weld should be located somewhere near Horizon 1, where underlying salt has evacuated and flowed south. The classical P-P seismic attributes of a salt weld are labeled on the data display:

- Events above the weld are usually discordant with events below the weld,
- The signal-to-noise ratio is often low in the data window that encompasses the weld, and
- Events below the weld tend to be lower frequency.

The radial P-SV image along this same profile is displayed as Figure 16. The vertical axis of this image space is labeled "warped P-SV time," meaning that P-SV image time has been adjusted to P-P image time, at least to a first-order level of accuracy. All P-SV data examples used in this discussion will be displayed as warped-time data. With P-P data and time-warped P-SV data displayed side by side, depth-equivalent geology can be recognized in P-P and P-SV image spaces with more confidence. The critical data needed to transform P-SV image-time coordinates to P-P image-time coordinates are Vp/Vs velocity ratios across the seismic image space. A single, space-invariant Vp/Vs function, shown in Figure 17, was used to transform P-SV image time to P-P image time across the total Shelf-B survey. This simplifying assumption that Vp/Vs behavior was laterally invariant over the large area spanned by Shelf-B data was made for expediency so that P-SV data could be compared quickly with P-P data. This assumption of spatially invariant Vp/Vs dependency causes the transformation of P-SV time to P-P time to have an embedded error that varies vertically and laterally across the survey; however, time-warped P-SV data are still adjusted to their companion P-P data to an accuracy that allows depth-equivalent P-P and P-SV structure and stratigraphy to be recognized.

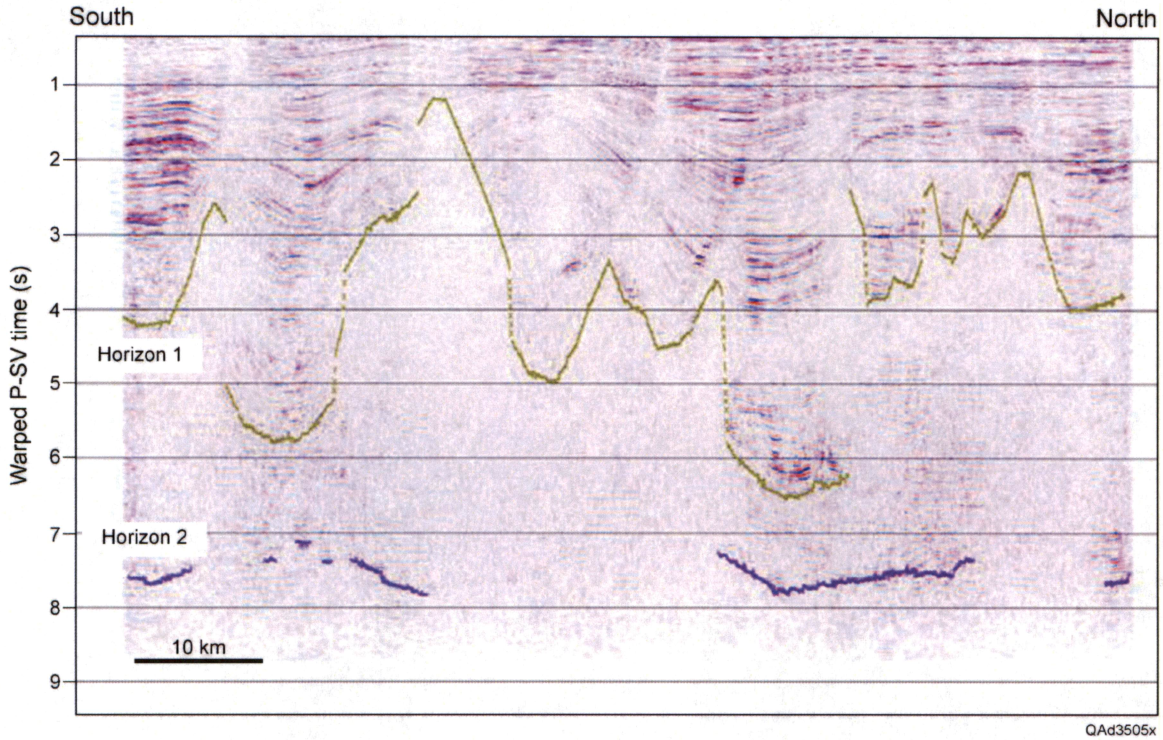

Figure 16. Radial P-SV image from the west portion of the Shelf-B survey. This image should be compared with its companion mode in Figure 15.

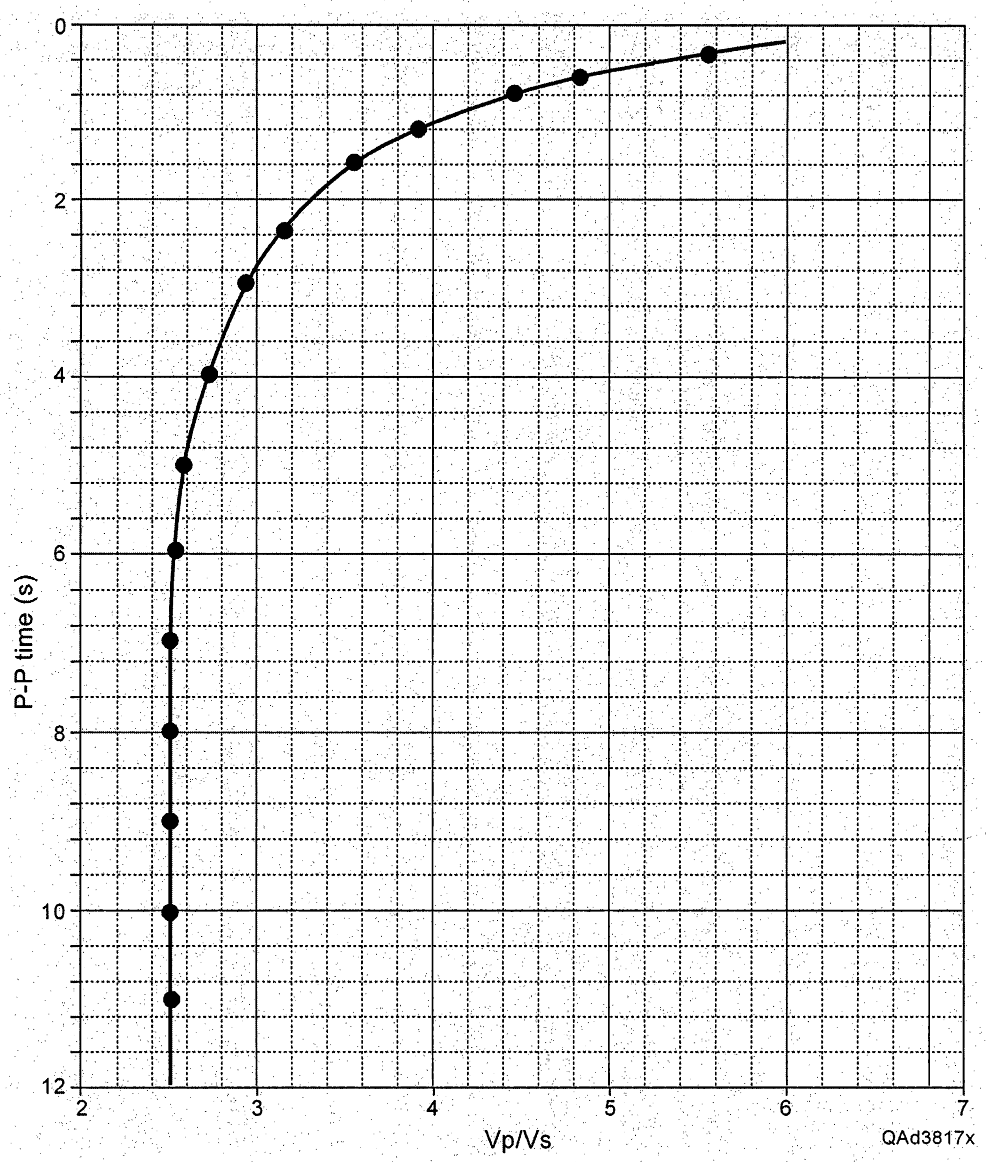

Figure 17. Time-variant Vp/Vs function used to transform P-SV image time to P-P image time.

Only the radial component of the P-SV wavefield will be used to illustrate the depth-imaging capability of these long-offset, P-SV data. For brevity, the adjective "radial" will be dropped when referring to these P-SV data.

The first P-SV image example is illustrated in Figure 16. If this image is compared with its companion P-P image (Fig. 15), P-SV Horizon 1 is approximately at the same image-time depths as P-P Horizon 1 (about 5 s) across the profile. Locally, P-P Horizon 1 and P-SV Horizon 1 differ. The important point is that in a broad perspective, the two horizons are essentially depth equivalent. This observation is a key principle. Many explorationists do not yet know how deep P-SV data can be applied. This data comparison provides critical information suggesting that P-SV data provide continuous, mappable reflections to the same depths as P-P data. A second point to emphasize is that local differences between P-P Horizon 1 and P-SV Horizon 1 are important only if these horizons are structural surfaces. Because the horizons are indicators of reflection quality (specifically indicating the base of deepest continuous reflections) and not structure surfaces, local differences between P-P Horizon 1 and P-SV Horizon 1 are not critical.

A different situation exists for Horizon 2. It is difficult to find any mappable P-SV events at image times significantly below P-SV Horizon 1. Only a few short segments of deep P-SV events are labeled in Figure 16. In contrast, the P-P data contain a large population of deep Horizon 2 events (Fig. 15). The lack of P-SV events near the super-deep depths of P-P Horizon 2 does not reduce the value of P-SV data for evaluating deep drilling targets in the GOM basin. The image times of Horizon 1, where good-quality P-SV reflections occur, will turn out to be the deepest depths that operators now wish to drill in this area of the GOM shelf.

A second data comparison is a north-south profile in the east part of the Shelf-B grid. P-P and P-SV images along this profile are shown as Figures 18 and 19. This profile is located about 60 mi (96 km) east of the profile shown in Figures 15 and 16. Comparison of these new P-P and P-SV images leads to the same conclusions as for the first profile, namely

- Good-quality continuous reflections extend down to 5 and 6 s for both the P-P and the P-SV modes (Horizon 1 in the figures),
- A thick section of sediment extending down to 10 s occurs in the north quarter of the profile,
- P-P data image deeper strata within the northern, thick, sediment mass than do the P-SV data, and
- The thick sediment load at the north end of the profile causes deep Jurassic salt to flow south and to form numerous salt structures and salt-driven, rotated fault blocks.

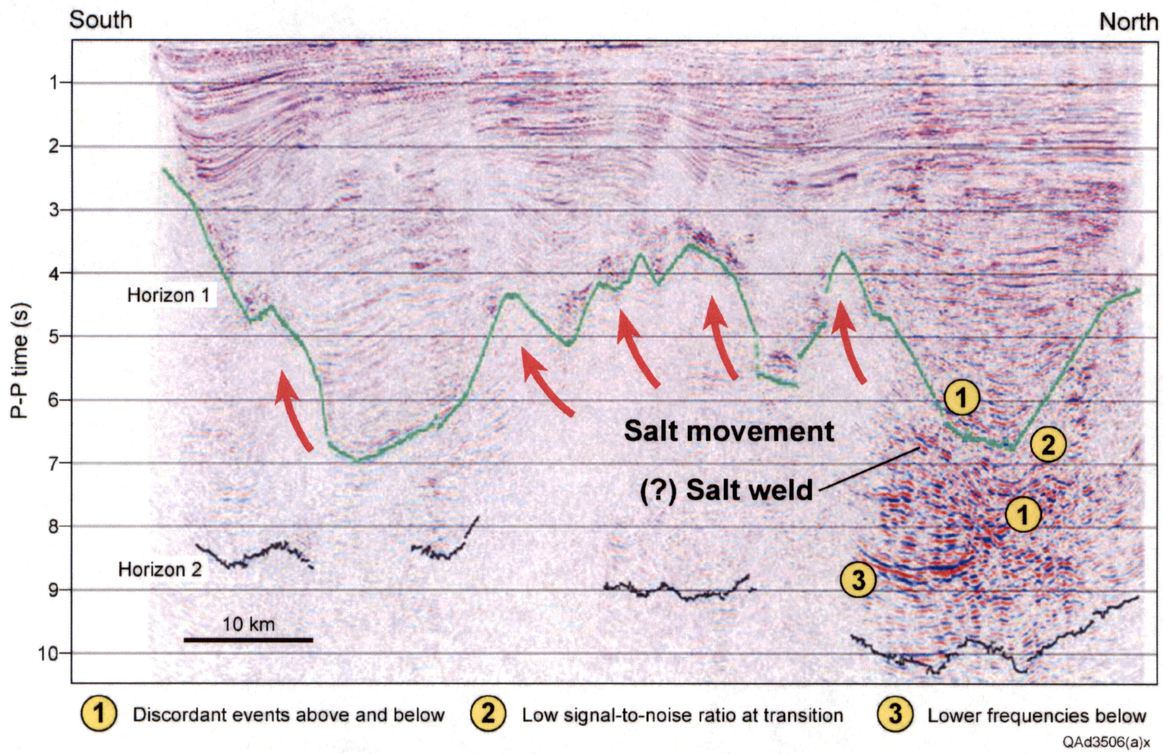

Figure 18. P-P image from the east portion of the Shelf-B survey.

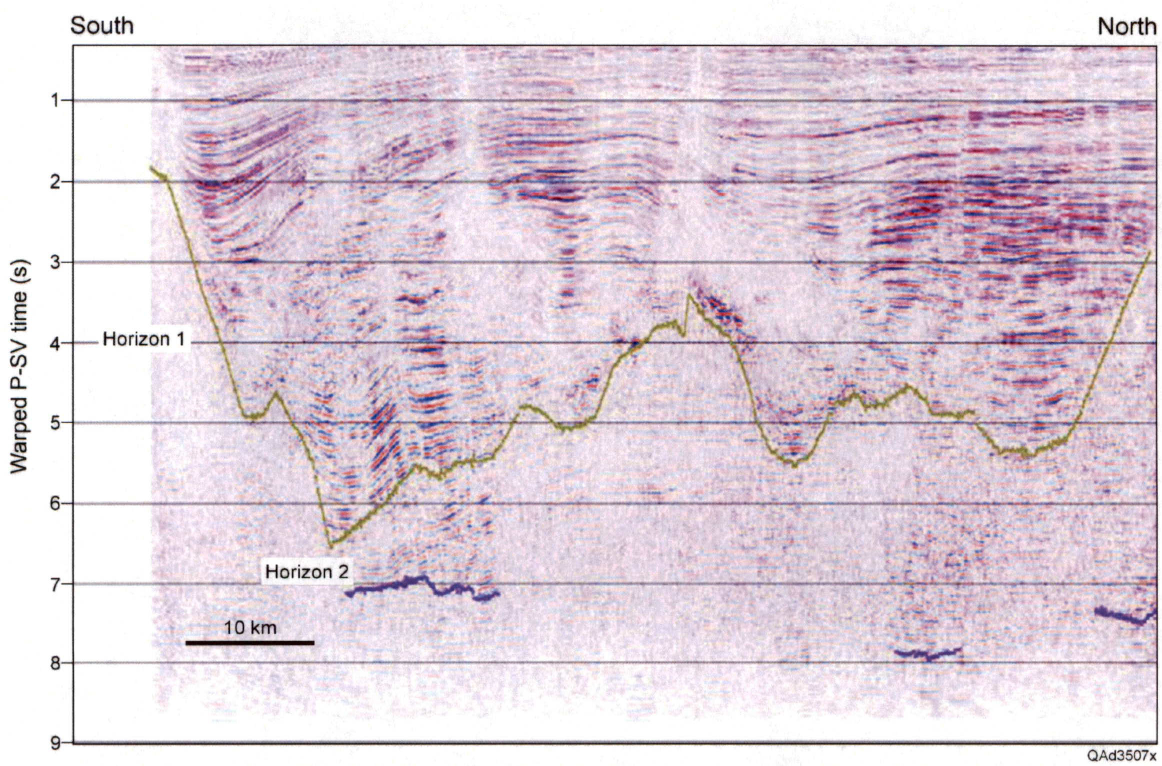

Figure 19. Radial P-SV image from the east portion of the Shelf-B survey. This image should be compared with its companion mode in Figure 18.

A third illustration of the deep-imaging capability of Shelf-B long-offset data is an east-west profile across the north part of the survey, where the two preceding profiles indicate that there is a thick sedimentary section extending to 10 s image time. The P-P and P-SV images produced along this profile are exhibited as Figures 20 and 21. This profile is about 75 mi (120 km) long. Again, a 10-km scale bar is added to each image to indicate the maximum source-receiver offset used in processing the data. The position of Horizon 1 on each image is subjective, as stated. Four interpreters at the Bureau of Economic Geology reviewed these data, debated where to position Horizon 1, and ended up with the surfaces positioned as shown in Figures 20 and 21. Note that good-quality P-SV reflections extend to deeper depths at the east end of this profile. Horizon 2 is rather definitive for the P-P data and oscillates between 9 and 10 s across the entire length of the profile. As was the case for the preceding north-south profiles, a deep Horizon 2 is difficult to find in the P-SV data. Short intervals of deep P-SV events are shown in Figure 21 at image times of 7 to 8 s, which places these reflections at depths of about 13 km (42,000 ft).

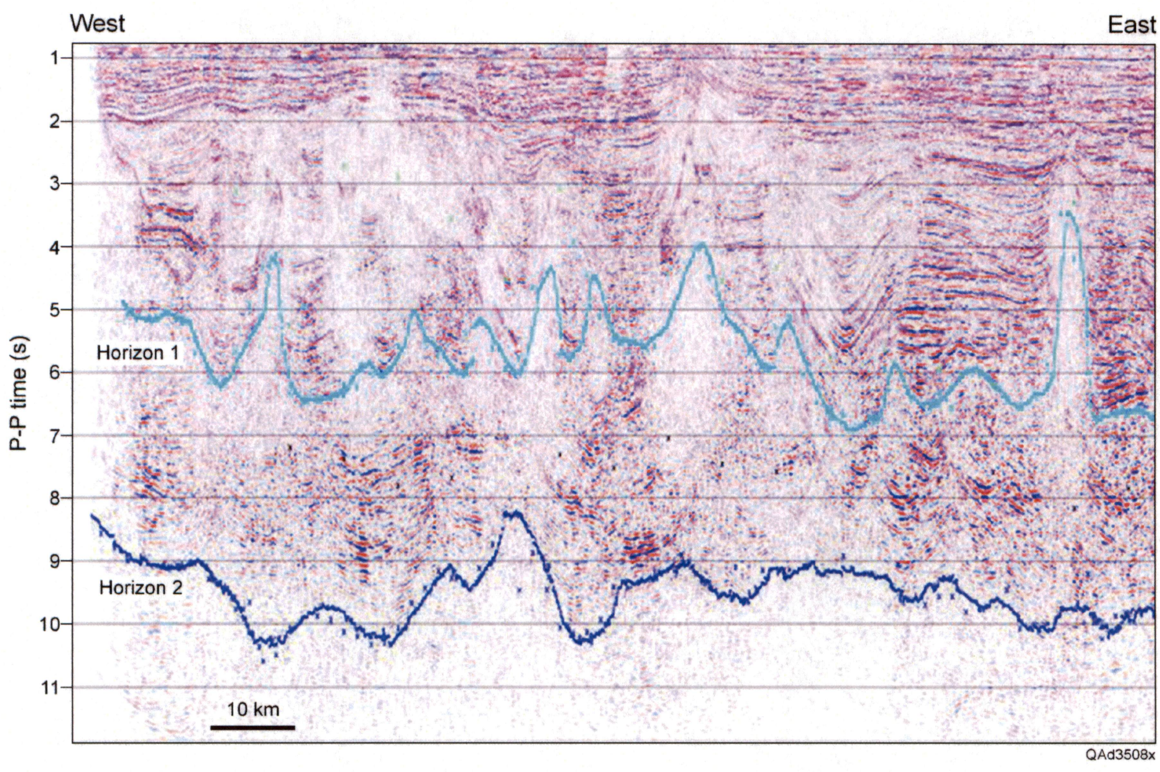

Figure 20. P-P image from the north area of the Shelf-B survey.

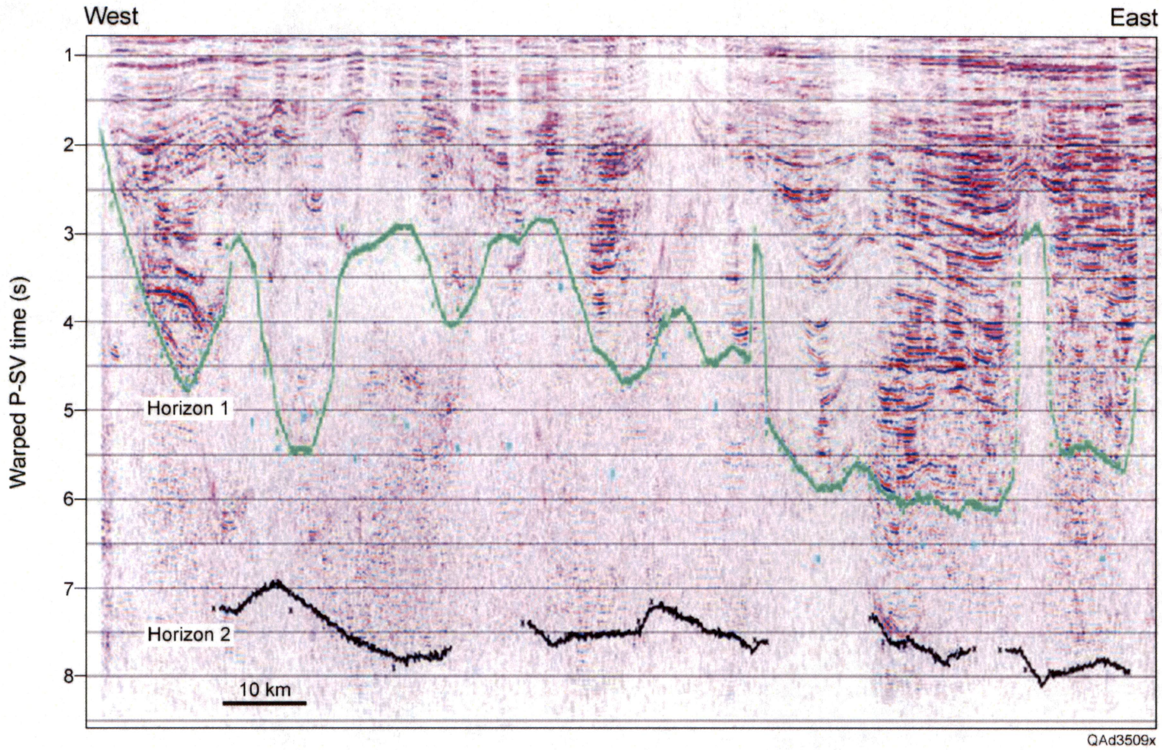

Figure 21. Radial P-SV image from the north area of the Shelf-B survey. This image should be compared with its companion mode in Figure 20.

P-P SEISMIC VELOCITIES

The time-based horizons in Figures 15 through 21 (Horizon 1 and Horizon 2) need to be converted to depth estimates for the depth-imaging capabilities of long-offset P-P and P-SV data to be better appreciated. The transformation from image time to depth was done using seismic interval velocities determined during seismic data processing. Examples of P-P rms interval velocities determined across the survey area are shown in Figures 22 and 23. Arbitrary north-south and east-west profiles are displayed to give a sense of the velocity behavior beneath the seismic grid. The deep velocity values on these profiles do not approach the Vp value of 7.6 km/s (23,000 ft/s) that Sawyer and others (1991) used to define the Moho. The velocity layering exhibits major vertical oscillations and thickness changes in the image-time interval between 3 and 6 s, where propagating wavefields first encounter salt-related structures.

The 10-km offset scale bar on each velocity profile is helpful for recognizing locations along the profile where lateral velocity variations occur over distances of the same dimensions as the positive-offset and negative-offset ranges used in data processing. Lateral velocity changes of this physical scale will complicate deeper imaging. Below 6 s, the velocity layering is reasonably smooth and uniform. All velocity layers drop deeper at the north end of the profile (Fig. 22), where the thickest sediment accumulation is encountered and little (no?) high-velocity salt is present.

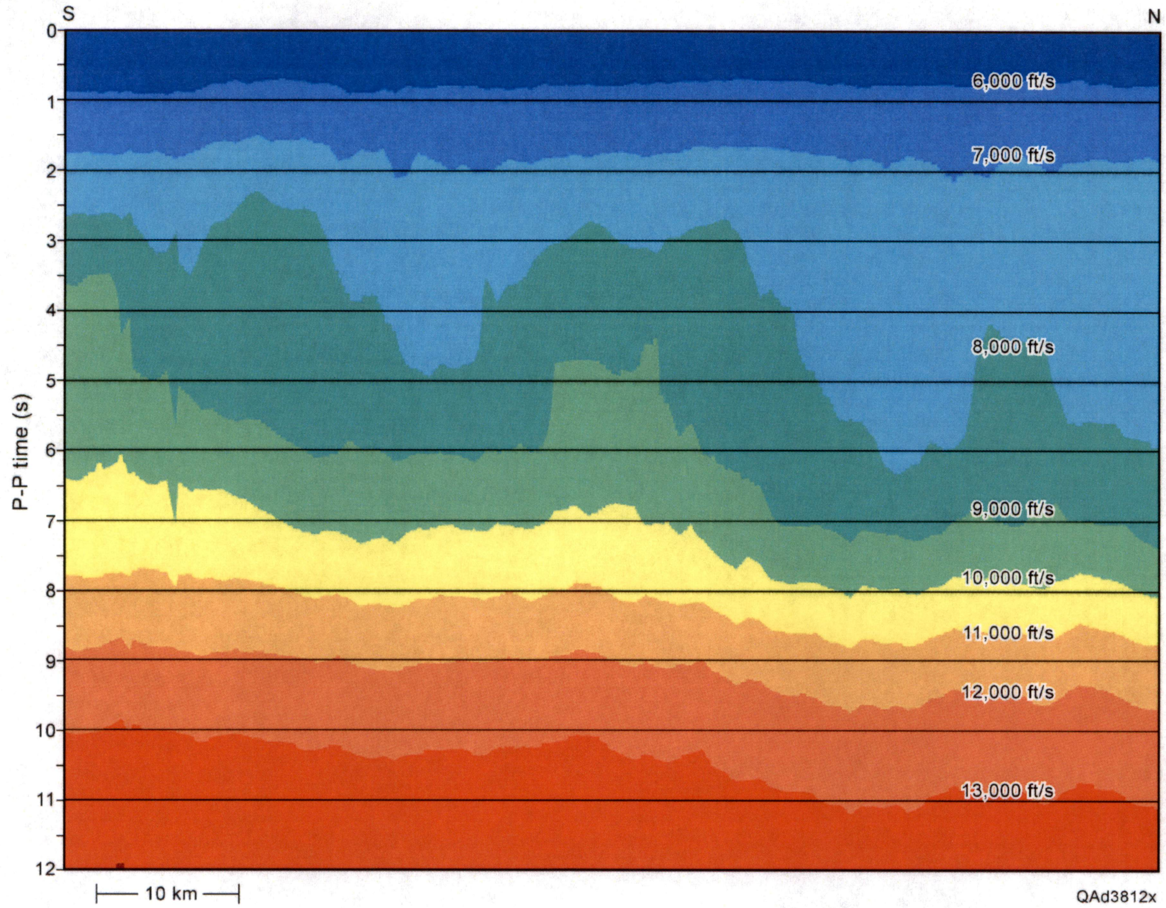

Figure 22. Arbitrary north-south profile showing P-P rms interval velocities across the area.

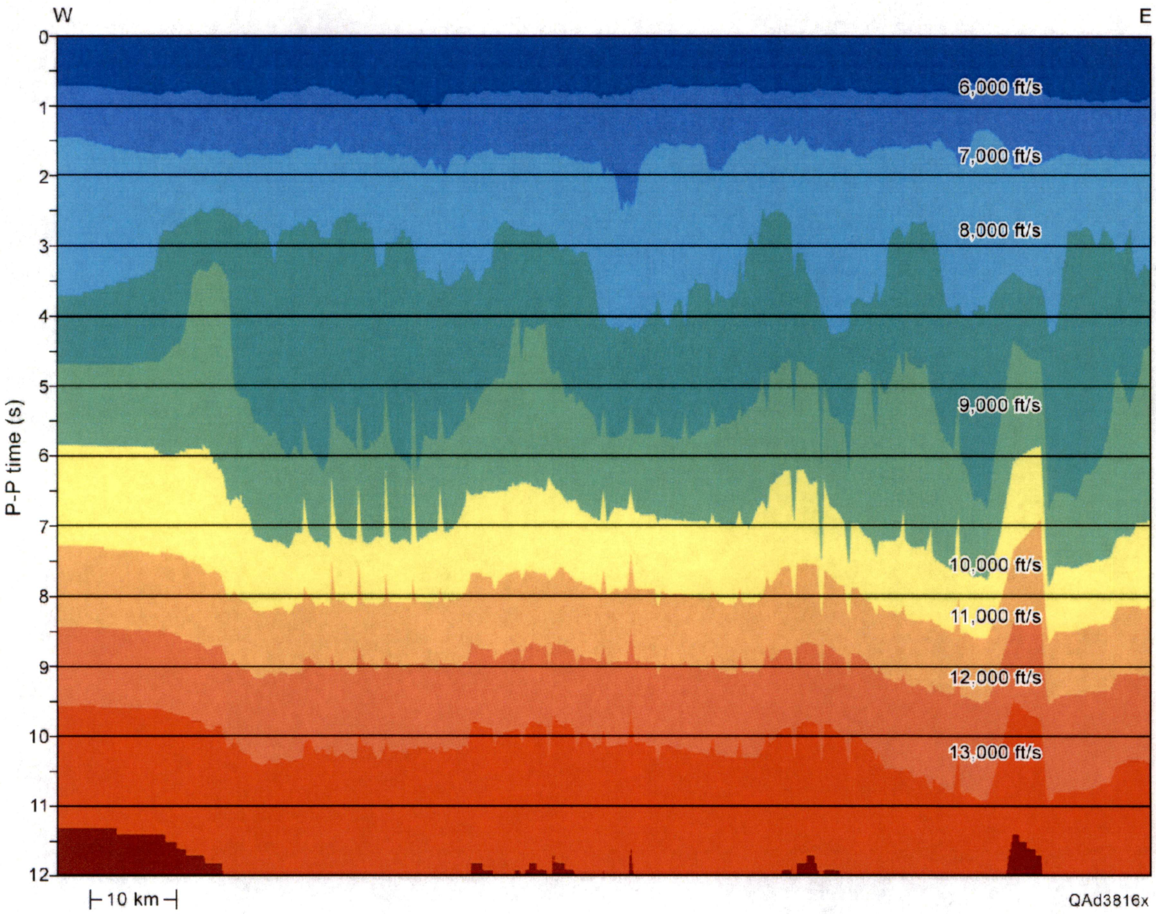

Figure 23. Arbitrary east-west profile showing P-P rms interval velocities across the seismic grid.

DEPTH ESTIMATES OF SEISMIC DATA QUALITY

The basic messages provided by depth conversions of P-P Horizon 1 and P-SV Horizon 1 are critical information for explorationists operating in the GOM basin. First, the depth conversion of Horizon 1 shows that long-offset 4-C OBC data can provide good-quality P-SV and P-P reflection images of GOM geology to depths of 30,000 ft (9 km). Second, the fact that good-quality, continuous P-P reflections extend down to 30,000-ft targets is not surprising. The fact that equivalent-quality P-SV reflections are obtained for these same target depths is new information.

SUPER-DEEP IMAGING

The Shelf-B long-offset seismic data provide a unique opportunity to image super-deep GOM-basin geology beneath the salt province where the Shelf-B survey is located. The illustration of this super-deep imaging will be limited to the P-P seismic mode because the preceding examples of image quality along selected Shelf-B profiles show that although the P-SV mode provides super-deep information, that information is restricted to smaller, more-segregated patches than is super-deep information provided by the P-P mode.

The depth conversion of the base of the super-deep P-P reflections (Horizon 2) shows that reflections from depths of 60,000 ft (18 km) occur beneath the Shelf-B survey. An east-west trend of 60,000-ft reflection depths extends across all of the north edge of the survey, corresponding to the deep 10-s image times of P-P Horizon 2 noted on the example profiles (Figs. 15, 18, and 20).

In summary, the Shelf-B long-offset data image strata in the GOM basin deeper than what previous investigators thought was possible. Conventional wisdom has been that deepest P-P reflections extend to 6 s and maybe 7 s (Figs. 11 and 13) and that the thickest sediment is about 15 km thick or maybe as much as 20 km (Figs. 7, 8, 9, and 14). The Shelf-B, P-P, long-offset data image to 10 s and show strata at depths of 18 km. Even the long-offset P-SV data image geology to depths of 7 and 8 s or 42,000 ft (13 km) in some areas, which is beyond the maximum image times and depths proposed by conventional wisdom.

IMAGING DEEP DRILLING TARGETS

Super-deep geology at the depths (60,000 ft) described by P-P Horizon 2 is beyond current drilling interest. Even the depths of deepest P-SV Horizon 2 reflections (~42,000 ft) exceed drilling depths planned by GOM operators. Most (all?) deep-drilling targets across the Shelf-B area of the GOM shelf are at depths near or above P-P and P-SV Horizon 1. Several examples of P-P and P-SV images at deep, but drillable, target depths will be illustrated in this section to document the quality and value of long-offset seismic data for evaluating deep GOM-basin geology.

This documentation will be done by positioning P-P and time-warped P-SV data side by side to aid image comparisons. In these data comparisons, either one feature (labeled A) or two features (A and B) in both image spaces are interpreted to be depth-equivalent and are highlighted. Comparing these labeled-letter features will demonstrate the accuracy at which time warping has adjusted the P-SV data to the same image-time coordinates as the P-P data. Several additional features across the P-P and P-SV image spaces will then be labeled with numbers (1, 2, 3, . . .). These labeled-number features emphasize some type of stratigraphic or structural information that is obvious in one image space but not in the companion image space.

Example 1 is chosen from the west part of the Shelf-B survey. The selected data window, displayed in Figure 24, has a base at a depth of about 5.5 km (18,500 ft). The dipping strata defined by reflection package A in each image space are interpreted to be depth-equivalent geology. In this instance, the spatially invariant time-warping function (Fig. 17) positions A about 200 ms too early in time-warped P-SV image space. Even so, depth-equivalent P-P and P-SV structure and stratigraphy can be identified between the two image spaces. Event 1 indicates stratigraphy that is better imaged by the P-P mode than by the P-SV mode. Events 2 through 5 are strata that are better imaged by the P-SV mode than by the P-P mode. The fact that one mode of a multicomponent seismic wavefield images stratal surfaces that are not seen by its companion wave modes is the attraction for acquiring multicomponent seismic data across a prospect area and is the basis of a new interpretation science, *elastic wavefield seismic stratigraphy*, being developed at the Bureau of Economic Geology.

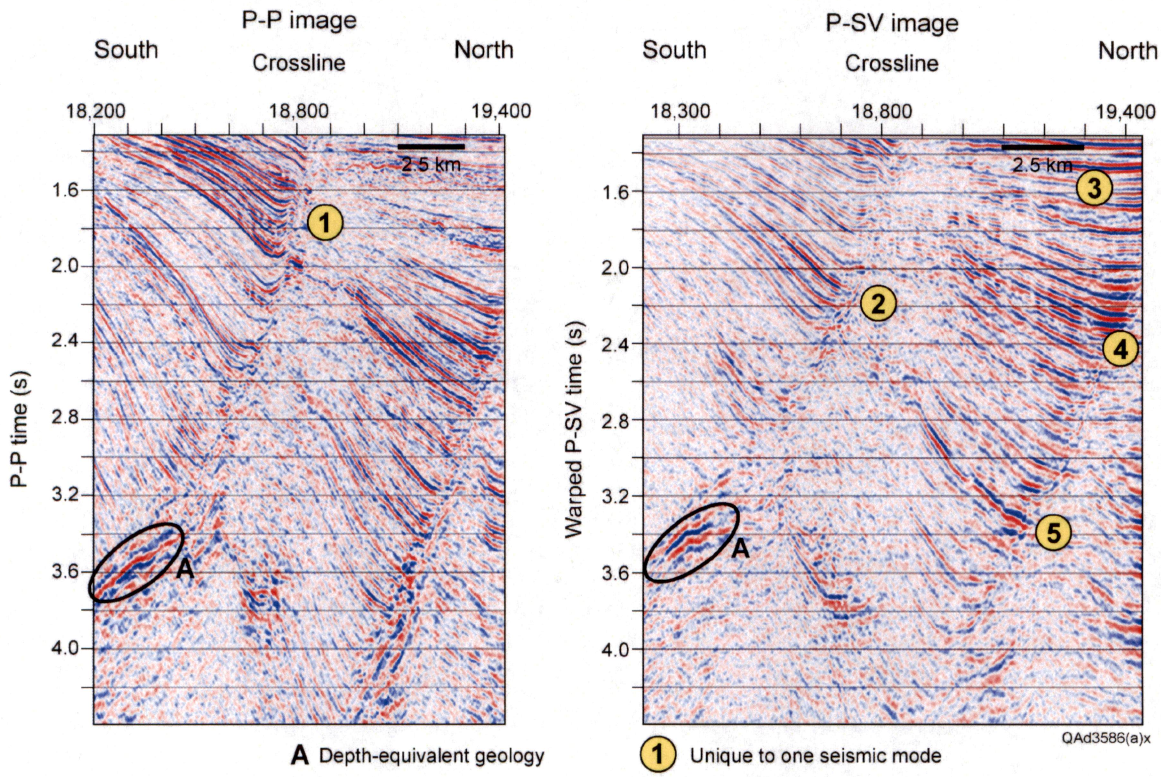

Figure 24. Comparison of deep, depth-equivalent, P-P and P-SV data windows in the west part of the survey.

Example 2 (Fig. 25) is from the central part of the survey. This data window extends to a depth of about 6.3 km (21,000 ft). The small anticline-like feature defined by reflection package A in each image space is interpreted to be depth-equivalent geology. Again, the time-warping function places event A in P-SV image space about 200 ms higher than where it is in P-P image space. Event 1 demonstrates an important aspect of P-P and P-SV wave physics for steep-dip imaging. Positive-offset P-SV data often provide an image of steep-dip strata that differs from the image provided by negative-offset P-SV data. In the processing of P-SV data, positive-offset data and negative-offset data are processed separately and imaged separately (Fig. 3). Near the end of the data-processing sequence, positive-offset and negative-offset images are summed to make a total-offset image. It is not uncommon for one of these half-offset P-SV images, either the positive-offset data or the negative-offset data, to image some steep-dip strata better than the other half-offset image does. Neither is it uncommon for this particular half-offset image to show the steep-dip target better than the total-offset image does. All P-SV images used in this discussion are total-offset images. Feature 1 in Figure 25 is an example in which a total-offset P-SV image does not depict steep dips in the same way as do P-P data. For a more acceptable depiction of structural dip to be inserted into P-SV image space, the solution is sometimes as simple as inspecting the positive-offset P-SV image and the negative-offset P-SV image and selecting the half-offset image that optimizes the P-SV steep-dip strata. This example may cause some interpreters to assume that CMP-based P-P data provide a more reliable image of dipping strata than do CCP-based P-SV data. However, a later example (Fig. 29) shows where P-SV data show dipping strata better than P-P data do.

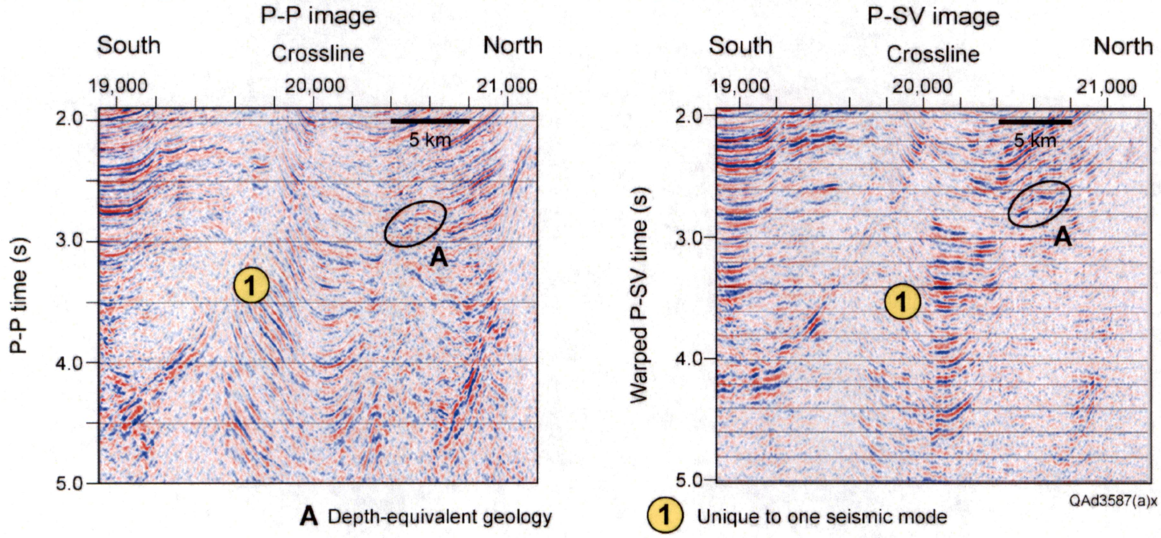

Figure 25. Comparison of deep, depth-equivalent, P-P and P-SV data windows in the central part of the survey. Compare this steep-dip imaging with that of Figure 29.

Example 3 is from the north part of the Shelf-B survey and is shown in Figure 26. The base of this data window is about 5.5 km (18,000 ft). Reflection packages A and B are interpreted to be depth-equivalent geology. Here the time warping places A and B in P-SV time-warp space within 100 ms of their positions in P-P image space. Interval 1 indicates sequence geometry that is better seen by the P-P data than by the P-SV data. Reflection sequences 2 and 3 are important examples because they document a situation in which P-SV data image deep geology better than P-P data do.

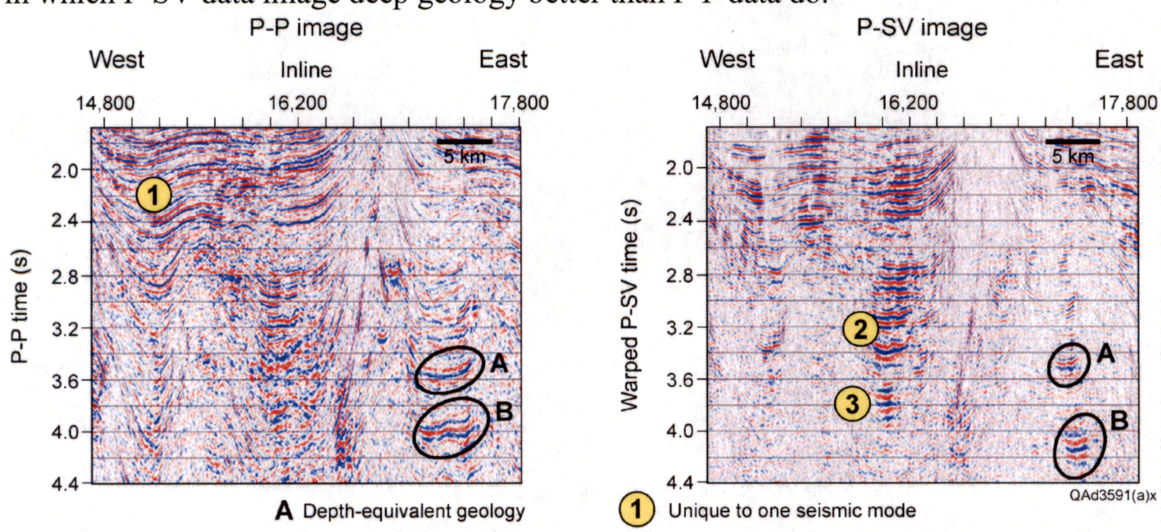

Figure 26. Comparison of deep, depth-equivalent P-P and P-SV data windows in the north area of the survey.

Example 4 is from a second area in the north part of the survey. The selected data window (Fig. 27) extends to almost 7.5 km (24,000 ft). Structural features A and B are interpreted to be depth-equivalent. The time-warping process positions A and B in time-warped P-SV space to within 100 ms of their positions in P-P image space. A narrow, vertical salt structure blanks out the deeper portions of the P-P and P-SV images about halfway between CDP coordinates 19,600 and 21,000. Features 1 through 4 on the P-SV image indicate a cyclic depositional process that is not obvious in the P-P image. Feature 5 is an example of P-SV data showing strata that are not present in the P-P data.

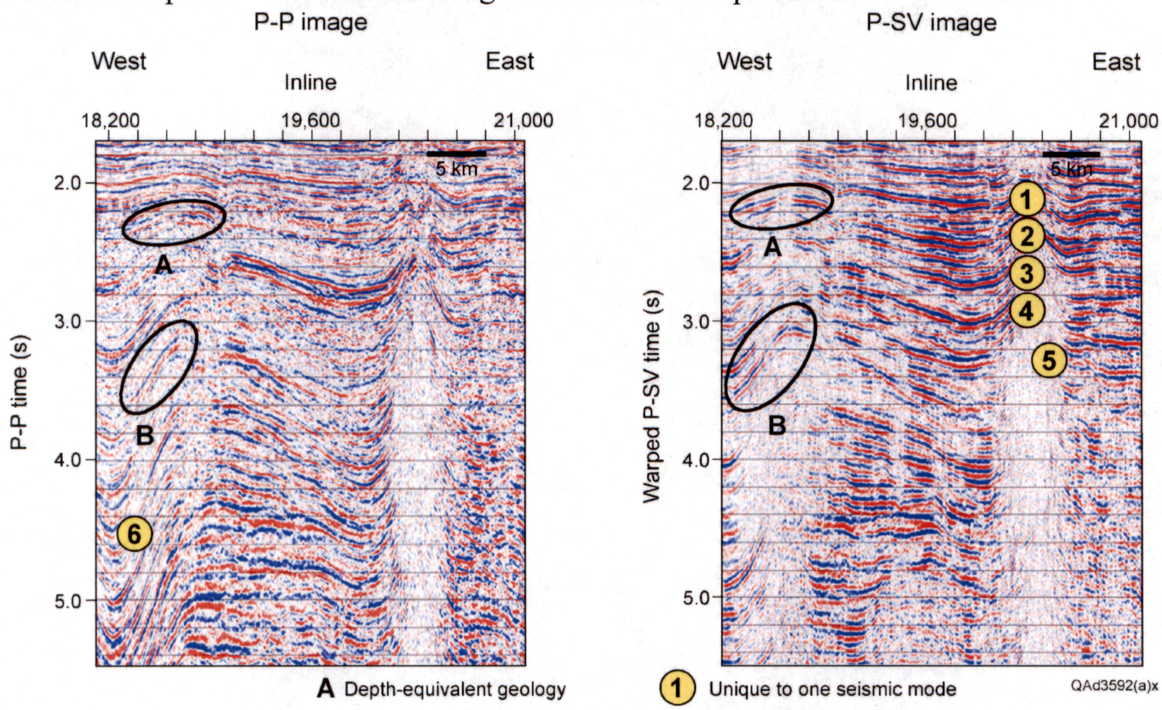

Figure 27. Comparison of deep, depth-equivalent P-P and P-SV data windows in the north area of the survey.

Example 5 in Figure 28 is from the south part of the survey and images to a depth of about 18,000 ft (5.5 km). Reflection package A labeled on each image is interpreted to be depth-equivalent geology. In this part of the survey, the time-warp transform is quite accurate, and reflection A is at the same image coordinate in both data spaces. High-amplitude event 1 in P-P image space is a pore-fluid variation that is absent in the P-SV image, as it should be. Strata packages 2 through 5 are examples of P-SV data imaging deep sequences better than P-P data do.

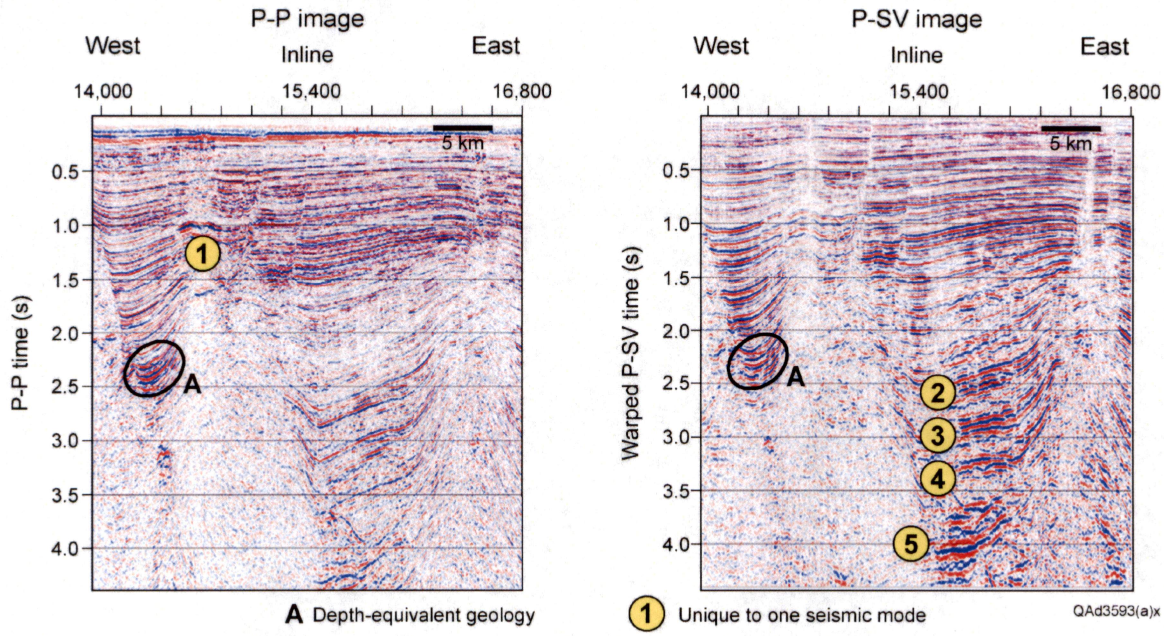

Figure 28. Comparison of deep, depth-equivalent P-P and P-SV data windows in the south part of the survey.

Example 6 is taken from a second target area in the south part of the survey and is shown as Figure 29. This data window is shallower, about 4 km (13,000 ft), and is not a "deep" target. However, these data show steep-dip imaging that is needed to balance the observations about steep-dip imaging that were made for example 2 (Fig. 25). Syncline features A and B are interpreted to be depth equivalent. The central part of each image is affected by a local salt structure. The P-SV image provides more geologic information east of this salt structure than does the P-P image, as indicated by labeled features 1 through 5. Note that in this case, the P-SV data image dips steeply on the east flank of the salt structure better than the P-P data do. This steep-dip imaging contrast between P-P and P-SV data is opposite that illustrated in Figure 25.

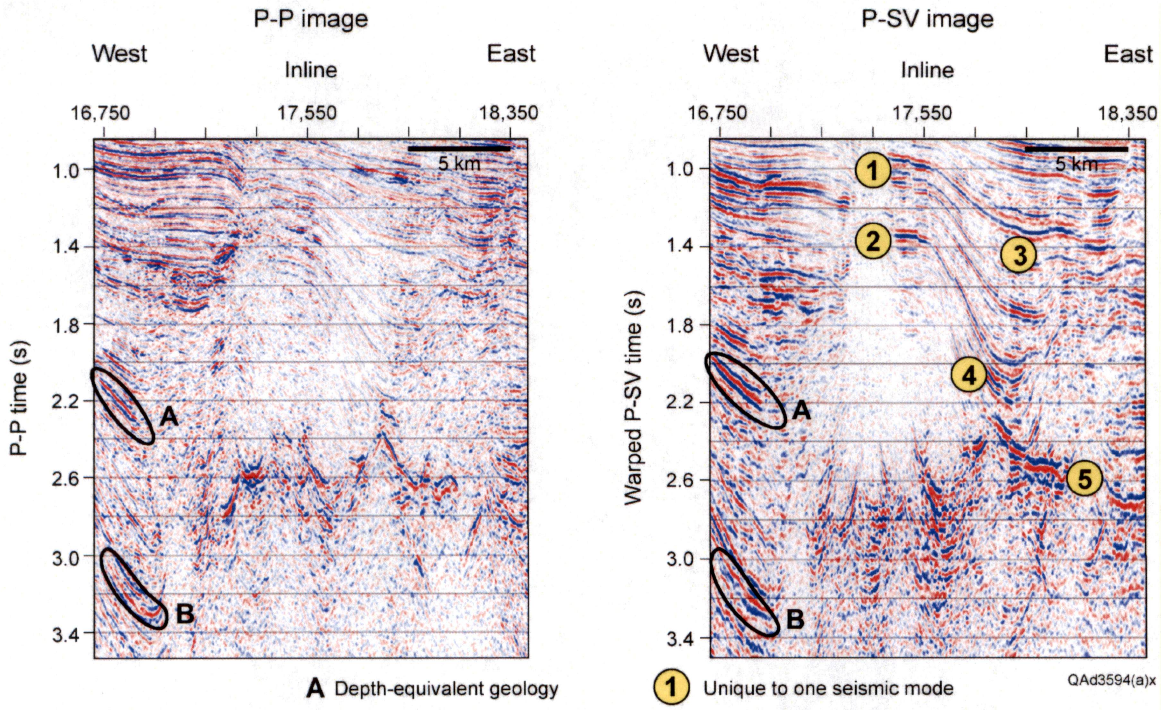

Figure 29. Comparison of shallower, depth-equivalent P-P and P-SV data windows in the south part of the survey. Compare this steep-dip imaging to that in Figure 25.

The last example is from the east side of the survey. This selected data window in Figure 30 extends to a depth of only 2.5 km (8,000 ft) and does not image deep geology. This shallow window was chosen because it contains an excellent example of the distinction between P-P seismic stratigraphy and P-SV seismic stratigraphy. Reflections A and B are interpreted to be depth-equivalent stratal surfaces. The time-warp transform positions A and B in time-warp P-SV data space at the same positions where they occur in P-P image space. P-SV features 1 and 2 define a sequence geometry that is absent in the P-P data. An interpreter using only P-P seismic data would construct a system architecture at this depth that differs fundamentally from the system architecture that would result if both P-P and P-SV data were used in a seismic-stratigraphy analysis. The fact that over some stratigraphic intervals, one seismic mode of a multicomponent seismic wavefield sometimes images different stratal surfaces, different seismic sequences, or different seismic facies than do other modes of that wavefield is the basis of the Bureau's research program, *Elastic Wavefield Seismic Stratigraphy.* Feature 3 is an example of the P-SV mode imaging other strata not easily seen in the P-P image.

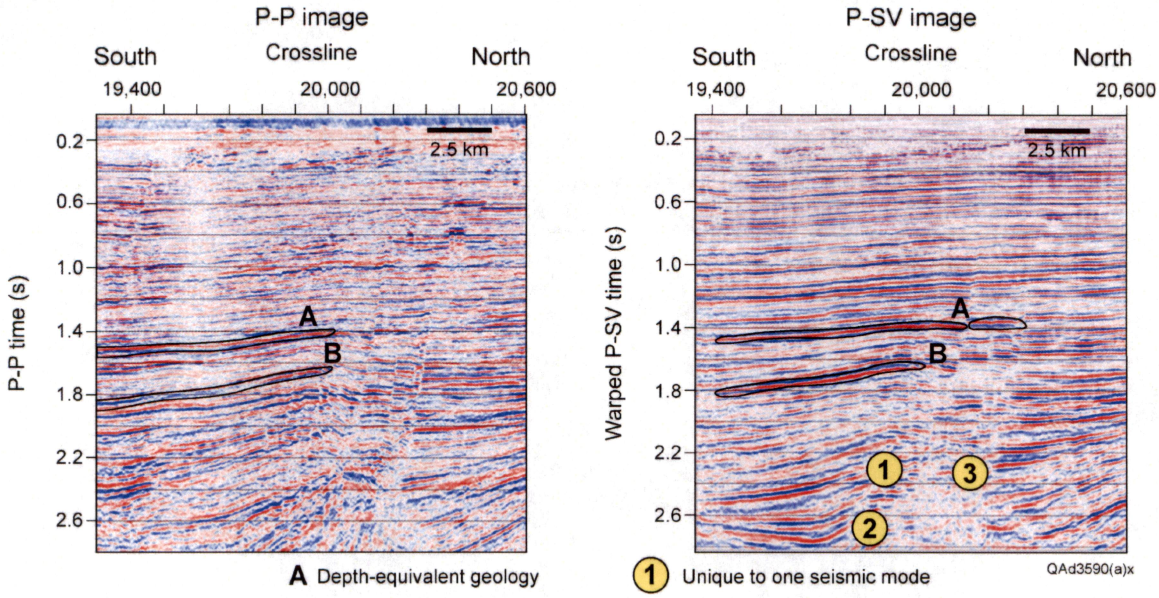

Figure 30. Comparison of shallow, depth-equivalent P-P and P-SV data windows in the east part of the survey. These data are a classic example of the principle of elastic-wavefield seismic stratigraphy.

CONCLUSIONS

Ocean-bottom-cable (OBC) seismic technology allows long-offset seismic data to be acquired across congested production areas where long-offset towed-cable seismic technology is not feasible. Further, 4-C OBC seismic technology provides both P-P and P-SV data. Towed-cable technology provides only P-P data.

This study focused on a large, 3,200-mi^2 (8,200-km^2) area of the Louisiana shelf, where 4-C OBC data were acquired and processed with source-receiver offsets of 10 km. This large-offset geometry provided data that image deeper than any previous seismic reflection data in the area. Analysis of these long-offset data shows that the P-P mode contains reflection signals from depths of 60,000 ft (18 km), which is deeper than any reported seismic reflection effort in the GOM basin. Equally important, the critical P-SV mode has reflection signal from depths of 42,000 ft (13 km).

Practical drilling targets across the Louisiana shelf are limited to depths of 30,000 ft (9 km) or less. Both long-offset P-P and long-offset P-SV data provide good-quality, continuous reflections to these depths. The documentation that P-SV images are of a quality equal to that of P-P images at these deep depths is new, important information. The study confirms that the fundamental requirement for good imaging of deep targets is acquiring long-offset seismic data. These research findings should encourage operators in the GOM basin to integrate long-offset 4-C OBC seismic technology into their prospect evaluations, particularly in areas where there are congested production facilities.

REFERENCES

Diegel, F. A., Karlo, J. F., Schuster, D. C., Shoup, R. C., and Trauvers, P. R., 1995, Cenozoic structural evolution and tectono-stratigraphic framework of the northern Gulf coast continental margin, *in* M. P. A. Jackson, D. G. Roberts, and S. Snelson, eds., Salt tectonics: a global perspective: AAPG Memoir 65, p. 109–151.

Exxon Production Research Company, 1985, Tectonic map of the world: available from American Association of Petroleum Geologists, Tulsa, OK.

Galloway, W. E., Bebout, D. G., Fisher, W. L., Dunlap, J. B., Jr., Cabrera-Castro, R., Lugo-Rivera, J. E., and Scott, T. M., 1991, Cenozoic, *in* A. Salvador, ed., The Gulf of Mexico Basin, Boulder, CO, Geological Society of America, The Geology of North America, v. J, p. 245–324.

Peel, F. J., Travis, C. J., and Hossack, J. R., 1995, Genetic structural provinces and salt tectonics of the Cenozoic offshore U. S. Gulf of Mexico; a preliminary analysis, *in* M. P. A. Jackson, D. G. Roberts, and S. Snelson eds., Salt tectonics: a global perspective: AAPG Memoir 65, p. 153–175.

Sawyer, D. S., Buffler, R. T., and Pilger, R. H., Jr., 1991, The crust under the Gulf of Mexico basin, *in* A. Salvador, ed., The Gulf of Mexico Basin, Boulder, CO, Geological Society of America, The Geology of North America, v. J, p. 53–72.